TÜRKİYE CUMHURİYETİ
ADANA ALPARSLAN TÜRKEŞ SCIENCE AND TECHNOLOGY UNIVERSITY

GRADUATE SCHOOL
ELECTRICAL AND ELECTRONIC ENGINEERING DEPARTMENT

DESIGN AND IMPLEMENTATION OF COMPLETELY SELF PROTECTED DISTRIBUTION TRANSFORMER

NİHAL GÜLŞAH KÖROĞLU

M.Sc.

ADANA 2024

TÜRKİYE CUMHURİYETİ
ADANA ALPARSLAN TÜRKEŞ SCIENCE AND TECHNOLOGY UNIVERSITY

GRADUATE SCHOOL
ELECTRICAL AND ELECTRONIC ENGINEERING DEPARTMENT

DESIGN AND IMPLEMENTATION OF COMPLETELY SELF PROTECTED DISTRIBUTION TRANSFORMER

NİHAL GÜLŞAH KÖROĞLU

M.Sc.

THESIS ADVISOR
ASSOC. PROF. DR. MURAT MUSTAFA SAVRUN

ADANA, 2024

DECLARATION OF CONFORMITY

In this thesis study, which was prepared following the thesis writing rules of Adana Alparslan Türkeş Science and Technology University Institute of Graduate School, I declare that I provide all the information, documents, evaluations and results in accordance with scientific ethics and moral codes without resorting to any means or assistance that would be contrary to scientific ethics and traditions. I also declare that I refer to all of the articles I used in this study with appropriate references and accept all moral and legal consequences if a situation is found contrary to my statement regarding my work.

24/01/2024

[Signature]

Nihal Gülşah KÖROĞLU

ÖZET

TAMAMEN KENDİNDEN KORUMALI DAĞITIM TRAFOSU TASARIMI VE UYGULAMASI

Nihal Gülşah KÖROĞLU
Yüksek Lisans, Elektrik-Elektronik Mühendisliği Anabilim Dalı
Danışman: Doç. Dr. M. Mustafa SAVRUN
Ocak 2024, 92 sayfa

Geleneksel dağıtım transformatörlerinde, sistemin korunması için ayırıcılar, kesiciler, parafudrlar, ölçüm panosu gibi ek donanımlar harici olarak monte edilmektedir. Kullanılacak transformatörlerin tipi, koruma elemanları ve diğer ek donanımlar ülkeden ülkeye değişiklik göstermektedir. Amerika, Meksika ve Hindistan gibi kimi ülkelerde elektrik enerjisi dağıtımının bir kısmı, ilk yatırım maliyeti düşüklüğü, daha esnek işletme koşulları, hızlı devreye alma gibi sağladığı avantajlar nedeniyle tamamen kendinden korumalı (CSP) transformatörler ile gerçekleştirilmektedir. CSP transformatörler, geleneksel transformatörlerde karşılaşılabilen bakım ve işletme problemleriyle karşılaşılmayan elektrik makineleridir. Bu transformatörler sekonder kısa devrelerden, yıldırım darbesinden, aşırı yüklenmelerden kendi kendini koruyabilmekte ve aşırı yüklenme durumu hakkında görsel uyarı verebilmektedirler. Bu makineler ayrıca arıza durumunda kendisini sistemden izole ederek bağlı olduğu dağıtım sistemini de korumaktadırlar. Bu tezde, 500 kVA, 33/0.4 kV CSP transformatörün tasarımı ve geliştirilmesi ele alınmıştır. Transformatörün elektriksel, termal, mekanik tasarımı detaylı olarak sunulmuş ve malzeme/ekipman seçimleri tasarım parametreleri hesaba katılarak tamamlanmıştır. Performans testleri aracılığıyla geliştirilen ürünün tatmin edici şekilde çalıştığı gözlemlenmiş ve deneysel doğrulaması yapılmıştır. Bu tez ile, CSP transformatörler ile ilgili literatüre katkı sağlayarak araştırmacılara ve transformatör üreticilerine ışık tutulması hedeflenmektedir.

Anahtar Kelimeler: dağıtım trafosu, elektromanyetik, tamamen kendinden korumalı dağıtım trafosu, tasarım, uygulama

ABSTRACT

DESIGN AND IMPLEMENTATION OF COMPLETELY SELF PROTECTED DISTRIBUTION TRANSFORMER

Nihal Gülşah KÖROĞLU
M.Sc., Department of Electrical and Electronic Engineering

Supervisor: Assoc. Prof. Dr. M. Mustafa SAVRUN
January 2024, 92 pages

In traditional distribution transformers, additional equipment such as load break switch, breakers, surge arresters and measurement panels are mounted externally to protect the system. The type of transformers, protection elements and other additional equipment to be used vary from country to country. In some countries such as America, Mexico and India, some of the electrical energy distribution is carried out with completely self-protected (CSP) transformers due to the advantages they provide such as low initial investment cost, more flexible operating conditions and rapid commissioning. CSP transformers are electrical machines that do not encounter the maintenance and operating problems that can be encountered in traditional transformers. These transformers can protect themselves from secondary short circuits, lightning strikes, overloads and provide visual warnings about overload conditions. These machines also protect the distribution system to which they are connected by isolating themselves from the system in case of malfunction. In this thesis, the design and development of 500 kVA, 33/0.4 kV CSP transformer is discussed. The electrical, thermal and mechanical design of the transformer is presented in detail and material/equipment selections are completed taking into account the design parameters. It has been observed that the developed product works satisfactorily through performance tests and its experimental verification has been made. With this thesis, it is aimed to shed light on researchers and transformer manufacturers by contributing to the literature on CSP transformers.

Keywords: distribution transformer, electromagnetic, completely self protected distribution transformer, design, implementation

Dedication

To my beloved family

ACKNOWLEDGEMENTS

I would like to express my deepest gratitude to my supervisor Assoc. Prof. Dr. M. Mustafa SAVRUN for his guidance, advice, encouragements and insight throughout this research.

I am also grateful to Assoc. Prof. Dr. Mehmet Uğraş CUMA and Assoc. Prof. Dr.Zehan KESİLMİŞ for accepting to be the member of defense committee.

I owe special thanks to Research Assistant Elanur EKİCİ for her companionship and cooperation during my study.

I would like to thank BETA Enerji ve Teknoloji Anonim Şirketi, for sharing the design data, production data, and test results of the transformer used in this study. I could not have completed this thesis without their support.

This thesis was financially supported by the Scientific and Technological Research Council of Turkey (TÜBİTAK) with a project number of 3191692.

Finally, I would like to express my deepest gratitude to my husband, Tahsin KÖROĞLU for her patience, encouragement and continuous morale support.

TABLE OF CONTENTS

LIST OF FIGURES

LIST OF TABLES

LIST OF ABBREVIATIONS

CSP	: Completely Self-Protected
AC	: Alternating Current
EMF	: Electromagnetic Force
IEC	: International Electrotechnical Commission
HV	: High Voltage
MVA	: Megavolt-Ampere
LV	: Low Voltage
HV	: High Voltage
AN	: Air Natural
AF	: Air Forced
AB	: Air Blast
ONAN	: Oil Natural Air Natural
ONAF	: Oil Natural Air Forced
OFAF	: Oil Forced Air Forced
OFAN	: Oil Forced Air Natural
ONWF	: Oil Natural Water Forced
OFWF	: Oil Forced Water Forced
PD	: Partial Discharge
HST	: Hot Spot Temperature
HVDC	: High Voltage Direct Current
HRGO	: Hot Rolled Grain Oriented
CRGO	: Cold Rolled Grain Oriented
MMF	: Magnetomotive force

LIST OF SYMBOLS

U_1	: Primary voltage
U_2	: Secondary voltage
E_1	: EMF induced in primary
E_2	: EMF induced in secondary
T	: Time
w	: Angular velocity
K	: Kelvin
°C	: Degree Celsius
N_1	: Number of primary turns
N_2	: Number of secondary turns
I_1	: Primary current
I_2	: Secondary current
a_1	: Sectional area of low-voltage conductors
a_2	: Sectional area of low-voltage conductors
f	: Frequency
ϕ_{max}	: Peak of the total magnetic flux
A	: Ampere
V	: Volts
δ	: Permissible current density
A_i	: Sectional area of core
B_m	: Maximum flux density in the core
K_i	: Stacking factor
A_w	: Window area
K_w	: Window space factor
A_y	: Yoke area
I_c	: Core loss component of no-load current
$\mathrm{Cos}\,\emptyset$	: Power factor

1. INTRODUCTION

The number of distribution transformer manufacturers is quite high both in our country and in the world for reasons such as being relatively easier to design and manufacture and low initial investment cost. This situation creates an important competitive environment and forces manufacturers to constantly develop new, efficient, low-cost, value-added products offered to the market by a small number of manufacturers. The purpose of this thesis was to meet these requirements. In some countries such as America, Mexico, Uganda, and India, electrical energy distribution is carried out with completely self-protected (CSP) transformers because of the advantages they provide, such as lower cost, more flexible operating conditions, and rapid commissioning.

In traditional distribution transformers, additional equipment, such as load break switch, breakers, surge arresters, and measurement panels, are mounted externally to protect the system. CSP transformers are electrical machines that do not encounter maintenance or operating problems that can be seen in conventional transformers. These transformers can protect themselves from secondary short circuits, lightning strikes, and overloads, and provide visual warnings about overload conditions. These machines also protect the distribution system to which they are connected by isolating themselves from the system in the case of a malfunction.

The aim of this thesis is to present the design, production, and performance analysis of an innovative CSP transformer. Within the scope of this thesis, CSP transformer design, prototype production, and tests were conducted. Excel was used to assign parameters following the completion of the AutoCAD drawings for the presented transformer. The design depends on the parameters defined in Excel, and the design automatically updates itself with every parameter change.

This study was handled in three stages. In the first stage, preliminary research and designs were carried out. Within the scope of the preliminary research activities, the specifications in the target markets where the products could be sold were examined in detail, and the product parameters were finalized. After the requirements were determined, design activities started. In this context, the mechanical, electrical and thermal designs of the transformer were carried out.

Because all components are located in the transformer, a design has been developed in a small volume without causing electrical stress or increasing magnetic losses.

In the second stage, the prototype manufacturing of the transformer, whose designs were completed, started. Subsequently, the windings and cores were manufactured. The transformer prototype was completed by combining the line breaker, internal fuses, cable box, and other protection equipment.

The prototype developed in the final stage was subjected to routine type and special tests. Within the scope of routine tests, measurement of winding DC resistance, measurement of short circuit losses and short circuit impedance, measurement of no-load losses and no-load current, measurement of no-load conversion ratio and control of polarity, applied voltage test, and induced voltage test were performed. Finally, in the type tests, the temperature increase and lightning strike tests were performed.

The CSP transformer developed in this thesis is the first product developed worldwide with rated values of 33 kV, 500 kVA rated values. When the relevant literature is examined, it is expected that the proposed transformer will become a pioneer. For secondary protection, unlike previous CSPs, circuit breakers will exist in a cable box on the transformer, whereas a line breaker and fuse pair will serve on the primary side. This approach will provide advantages over other similar products.

The advantages of the CSP transformer are summarized as follows.

- The transformer is self-protecting and does not require an external protection system. Thus, it has emerged as a plug-and-play solution.
- It is not affected by long-term overload situations that are not detected by conventional protection systems, owing to the thermal protection system. Owing to these features, they can operate at overload until the oil temperature reaches a temperature that strains the windings, thus providing longer service than conventional transformers.

- Because the transformer isolates itself from the distribution system to which it is connected in case of a fault, only the loads it feeds are affected, and it does not pose any problem to the rest of the system.
- As surge arresters are located directly on the transformer boiler, they are effectively protected from lightning strikes.
- Because the protection systems in CSP transformers are integrated into the product, they can be operated quickly and simply.
- Since the transformer is hermetic type, it does not absorb moisture.
- The condition of the signal lamp that can be placed on it is examined, and it informs the distribution system operator that it needs to switch to a higher power.

This thesis contributes to the field of power distribution by introducing a pioneering approach for transformer design and protection. These findings highlight the advantages of a Completely Self-Protected Distribution Transformer in terms of reliability, efficiency, and sustainability, paving the way for its potential integration into modern electrical grids. As the world continues to evolve towards an electricity-dependent future, CSP transformers are emerging as a promising solution for addressing the evolving challenges of power distribution systems.

1.1. Transformers

Machines that change voltage and current values in a ratio according to need without changing the frequency through electromagnetic induction are called transformers. Transformers are one of the basic building blocks of electricity transmission networks. Significant advances have been made in transformer technology as a result of the increasing need for reliable and safe electrical power distribution systems [1].

One of the most important features of electrical energy is that it can be easily transported to areas far from where it is produced. In order for this transport to be carried out efficiently, the voltage must be large enough. As it is known, electrical energy is produced as direct or alternating current. High voltage energy transmission in direct current has gained great importance recently. However, the desired level has not been reached in this regard. On the other hand, since the voltage of alternating current electrical energy is increased and decreased with the help of transformers, transportation of energy with alternating current maintains its importance [2].

Transformers, as an electrical machine used to lower or raise the power and frequency of alternating current without changing it, have an important place in the transportation of electrical energy in AC. Transformers are made of thin sheets and consist of two coils placed on the iron body, wrapped with insulated conductors with a closed magnetic circuit called the iron body. Except for auto transformers, these two coils are completely electrically insulated from each other.

Various applications for transformers can observed in railways and transportation installations [3, 4], commercial and residential buildings [5], industrial areas [6, 7], and electric transmission and distribution systems [8]. Hence, they can be divided into different categories based on their core shape, winding type, core material, kind of usage, power rating, transformation ratio, cooling type, etc.

1.1.1. Types of transformers

Transformers are vital electrical devices that can be classified into several types based on their intended applications, construction, and voltage levels. Classification of transformers according to their features is illustrated in Figure 1.

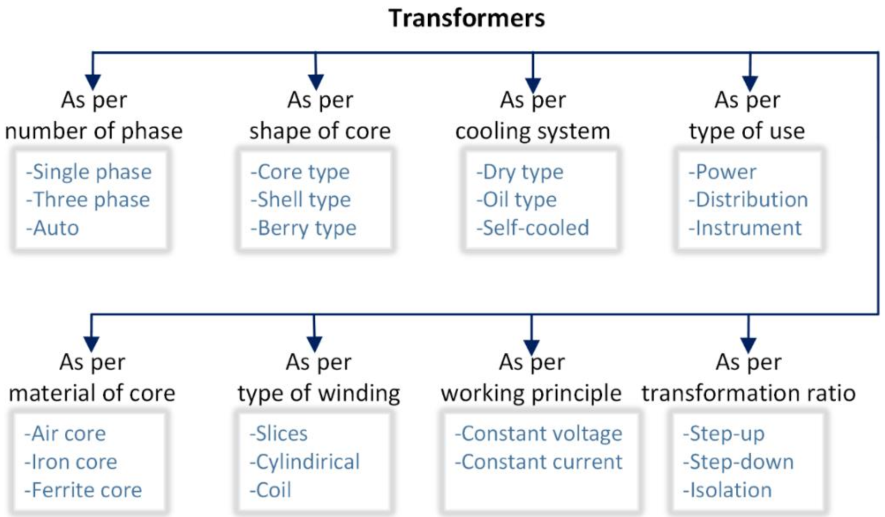

Figure 1.1. The classification of transformers.

Each type of transformer serves a unique purpose within the realm of electrical systems, adapting voltage levels and currents to meet the demands of various applications and industries. Understanding the characteristics and applications of these transformers is crucial for efficient and reliable electrical power distribution and utilization. Transformer types that we frequently encounter in practice are listed below:

- Transmission transformers,
- Distribution transformers,
- Power transformers,
- Autotransformers,
- Isolation transformers,
- Audio frequency transformers,
- Control transformers,
- Measurement transformers.

Transmission transformers are of high power (MVA) and are used as voltage boosters to transmit very high voltage to distant places. While intermediate station transformers are used to reduce the voltage to medium levels, distribution transformers are used to reduce the voltage from intermediate levels to lower intermediate levels and are large power transformers. Power transformers are used in electronic circuits and have many different types and applications. Autotransformers are generally used to provide a regulated voltage in low power applications.

Isolation transformers are transformers with equal input and output voltages and are used to isolate direct current. Even though the voltage applied to the primary contains both direct and alternating current components, the secondary voltage will consist of only the alternating component. That is, the direct current component will not be transferred to the output voltage. Isolation transformers are also used to isolate the noise that may occur between electronic circuits and the ground line.

Audio frequency transformers are used for impedance matching between amplifiers or at the output or input of audio frequency (up to 20 kHz) amplifier circuits. Control transformers are used to provide the desired adjustments in the amplitude and phase of the voltage at different points of the electrical system in circuits that require constant current or constant current at low power or VA values. Finally, measurement type transformers are placed to provide a safe connection between the high-energy part of the system and measurement instruments (various protection equipment such as ammeter, voltmeter, wattmeter and relays) and to monitor high voltages/currents [9].

The most commonly used transformer types of according to the purpose of use are power transformers and distribution transformers. Power transformers and distribution transformers are integral components of electrical systems that play pivotal roles in ensuring efficient and reliable electricity transmission and distribution. These two distinct types of transformers serve critical functions in the modern power grid, each tailored to address specific voltage levels and operational requirements.

Power transformers are primarily responsible for stepping up or stepping down voltage levels in high-voltage transmission networks, enabling the long-distance transmission of electricity from power plants to substations. On the other hand, distribution transformers function at lower voltage levels, facilitating the final transformation of electricity before it reaches homes, businesses, and industrial facilities. The hermetically sealed oil-type distribution transformer is shown in Figure 1.2.

Figure 1.2. Hermetically sealed oil-type distribution transformer.

Figure 1.3 depicts a dry-type distribution transformer, while Figure 1.4 shows an air-cooled distribution transformer.

Figure 1.3. Dry-type distribution transformer.

Figure 1.4. Air-cooled distribution transformer.

This thesis explores the fundamental principles, design considerations, operational characteristics, and maintenance strategies of distribution transformers, highlighting their significance in the broader context of electrical power systems. Through an in-depth examination of these essential components, this research aims to contribute to a deeper understanding of transformer technology and its crucial role in ensuring the reliability and sustainability of modern electrical grids.

1.1.2. Working principle of a transformer

As seen in Figure 1.5, there are two windings in a simple transformer, these are the primary winding and the secondary winding. The primary winding is the winding to which voltage is applied in the transformer. In the step-down transformer, it is wound with a thin section conductor with multiple turns, while in the step-up transformer it is wound with a thick section conductor with few turns. The secondary winding is the winding from which voltage is received. In the step-down transformer, it is wound with a thick section conductor with low turns. In the step-up transformer, it is wound as thin-section multi-wire.

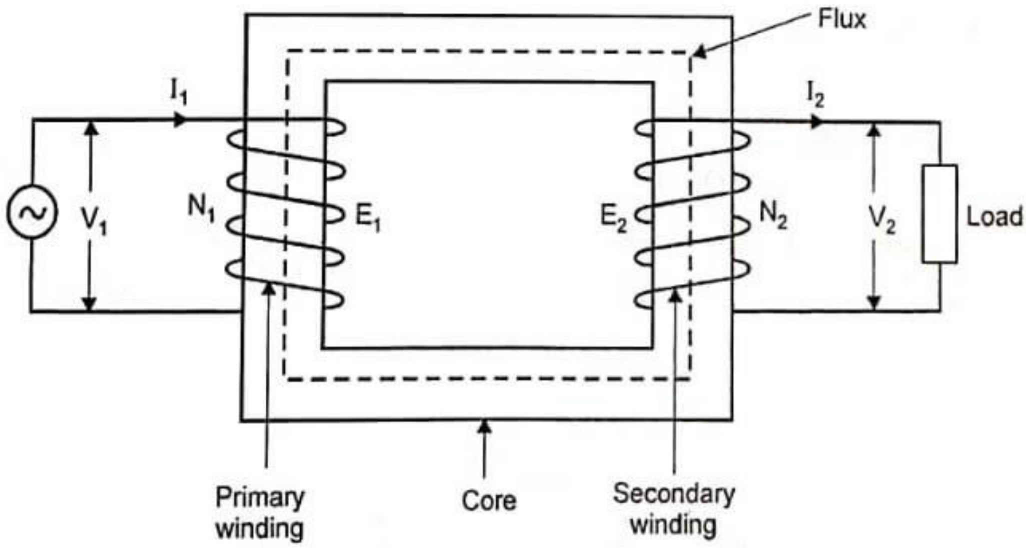

Figure 1.5. Working principle scheme of single-phase transformers.

The general operating principle of transformers is examined for operating situations where alternating voltage is applied and direct voltage is applied. If alternating voltage is applied, an alternating current flows through the primary windings. This I_1 current creates a magnetic field on the iron core, whose intensity and direction changes with time. This magnetic field completes the circuit by passing through the core and the leg where the secondary winding is located. The variable magnetic field force lines completing the circuit cut the secondary winding conductors and an electromagnetic force (EMF) is induced in the secondary windings. Thus, even though there is no electrical connection between them, the alternating voltage applied to the primary winding induces a voltage of the same frequency in the secondary winding via electromagnetic induction.

If direct voltage is applied to the transformer in Figure 1.5, a direct current flows through the primary winding and a magnetic field occurs on the core. However, this magnetic field is a constant magnetic field whose direction and intensity do not change. Since the secondary winding remains in the constant magnetic field, no EMF is induced on it. On the other hand, a change occurs when the correct voltage is applied and cut off. As a result, EMF is induced in the secondary winding for a short time. If an electronic circuit element called a vibrator, which frequently opens and closes the circuit, is placed in the primary winding circuit to which we apply direct voltage, alternative voltage can be obtained from the secondary winding, as it will be as if an alternative voltage has been applied to the primary windings. As a result, in order to receive voltage from the secondary in transformers, a voltage-current that changes direction and intensity according to time must be applied to the primary. If it is not applied, it is not possible to get a continuous voltage from the secondary. The EMF induced in single-phase transformers is generally expressed as follows [10]:

$$E = 4,44\, f\, \phi_{\max} N_1 \cos wt \tag{1.1}$$

Using this formula, the following expressions can be written for primary and secondary voltages.

$$U_1 = 4,44\, f\, \phi_{\max} N_1 \cos wt \quad \text{(primary voltage)} \tag{1.2}$$

$$U_2 = 4,44\, f\, \phi_{\max} N_2 \cos wt \quad \text{(secondary voltage)} \tag{1.3}$$

The voltage induced per turn is as follows:

$$U_s = \frac{U_1}{N_1} = \frac{U_2}{N_2} \tag{1.4}$$

The relationship between the primary and secondary voltages, currents and number of windings of the transformer is called the turns ratio. Every transformer has a fixed transformation ratio. Its formula is shown in Equation 1.5.

$$n = \frac{U_1}{U_2} = \frac{N_1}{N_2} = \frac{I_2}{I_1} \tag{1.5}$$

In the values in the formula, E_1 is the EMF induced in the primary, E_2 is the EMF induced in the secondary, U_1 is the voltage applied to the primary, U_2 Voltage taken from the secondary (Volts), N_1 number of primary turns, N_2 number of secondary turns, I_1 primary current (Amperes), I_2 secondary current (Amperes), n is the transformation rate, f is the frequency (Hz), $\phi_{\max}$ is the peak of the total magnetic flux, and $w = 2\pi f$ (rad/sec).

1.1.3. Transformer losses

The term "loss" in any electrical machine refers to the difference between the input and output powers. Since there are no moving or rotating parts in transformers, there is no friction or wind loss. However, various losses may occur in the windings and core material. The types of losses occurring in the windings and core of a transformer can be listed as follows: iron losses (core losses), copper losses (winding losses), stray loss, dielectric loss, hysteresis loss and eddy current losses. The classification of transformer losses is shown in Figure 1.6.

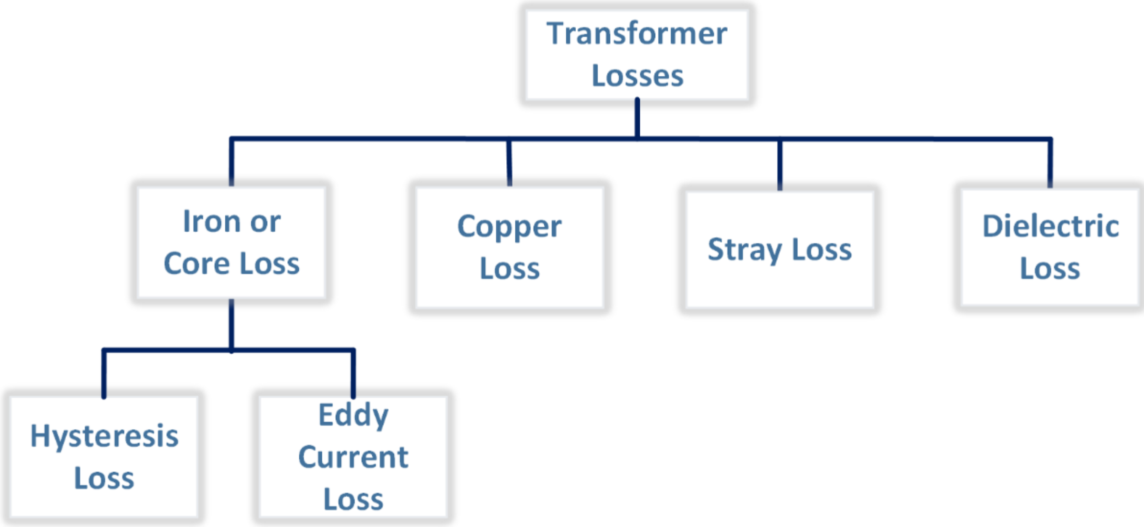

Figure 1.6. Classification of transformer losses.

1.1.3.1. Iron losses

It occurs due to the variable flux occurring in the core of the transformer. Iron losses, also known as core losses, are divided into two groups: hysteresis and eddy current losses. Hysteresis losses are losses that occur due to the changing magnetic field in the transformer core. As the magnetization of the core changes, the magnetic fields also change. The resistance encountered during this change causes energy loss. Additionally, as the magnetic field decreases, the magnetic flux does not decrease at the same rate. The magnetizing force must also be applied negatively in order for the flux density to be zero. The part within the hysteresis curve area given in Figure 1.7 below shows the energy loss.

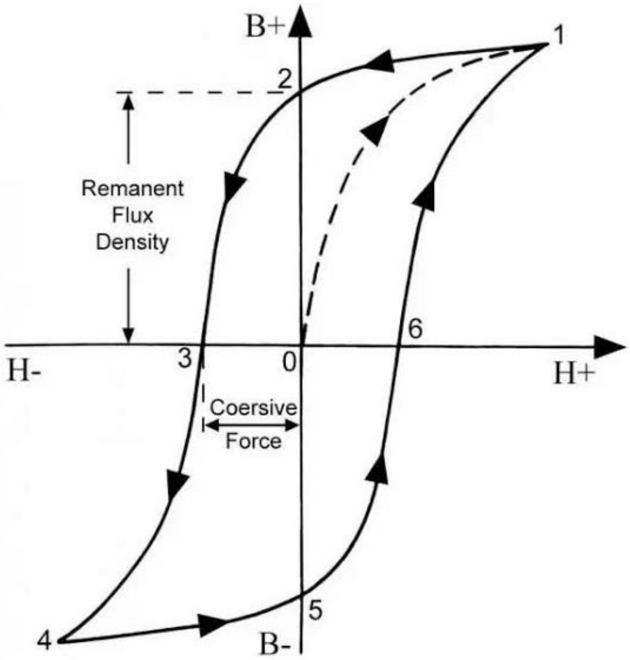

Figure 1.7. Hysteresis curve [11].

Eddy current losses occur due to Faraday's law, "If the current is passed through a wire, voltage is induced." Eddy currents arising from any variable and insignificant magnetic field in the transformer core cause energy loss. In accordance with the I^2R principle, they are released as heat. Transformers are made in the form of thin plates instead of single castings to prevent heating due to Eddy losses.

1.1.3.2. Copper losses

It is not possible for transformer coils to be pure inductive because they have ohmic resistance resulting from their own structure. Due to this resistance, copper losses occur in the transformer. The amount of loss also changes depending on the variability of the current. The total copper loss occurring in the primary and secondary winding is calculated as follows.

$$P = I_1^2 R_1 + I_2^2 R_2 \tag{1.6}$$

1.1.3.3. Stray losses

These losses occur in windings and metal parts. It got its name as stray because it can occur anywhere. Stray losses occur due to magnetic flux and magnetic field. Transformer design in large transformers is very important in preventing such losses. The less the leakage, the more efficiency will increase. It is smaller than iron and copper losses.

1.1.3.4. Dielectric losses

These are the losses that occur in the insulation of the transformer due to high electrical voltages. Efficiency decreases when there is any damage or wear to the oil or insulation of the transformer. In small diameter transformers, these losses are negligible compared to large losses.

1.2. Background and research motivation

In light of the literature review, it was seen that there are few studies on CSP distribution transformers. This study was carried out both to fill this gap mentioned in the literature and to guide transformer manufacturers. In this thesis, the design and implementation of a novel and pioneering CSP distribution transformer is addressed. Three basic steps will be followed, namely the design, implementation and testing of the proposed CSP transformer. A Macro-based Excel design program will be used in the design and theoretical calculations. CSP distribution transformer aims to enhance efficiency, safety, and reliability while simplifying operation and maintenance.

1.3. Objectives of the thesis

The aims of this thesis are listed below:

- Presenting a literature review about distribution transformers and CSP distribution transformers,
- Design and development of a prototype of 500 kVA, 33/0.4 kV CSP distribution transformer,
- Development of line breakers at 33 kV level,
- Completion of performance tests of CSP distribution transformer,
- Creating a product family with high added value and volume sales potential,
- Making publications as a result of the studies carried out.

The accessories in the prototype of the CSP transformer will be as follows:

- High voltage bushings and low voltage bushings
- High coltage off-load tap changer
- Pressure safety valve
- Hermetic protection relay
- Fuses
- Thermal magnetic circuit breaker
- Interrupter
- Current transformers
- Power analyzer

1.4. Outline of the thesis

The thesis's outline is arranged as follows:

- Chapter 1 provides general information about power and distribution transformers. In addition, the main stages of the study are addressed.
- A thorough literature review regarding distribution transformers and CSP transformers is presented in Chapter 2.
- Design considerations and prototype implementation details of the suggested transformer are introduced in Chapter 3.
- The results of the experimental studies and the discussions are described in Chapter 4.
- Finally, significant findings and the study's primary contributions are emphasized in Chapter 5.

2. LITERATURE SURVEY

Transformers have a long history dating back to the early 1880s. Power transformers with 400 kV ratings were manufactured as early as 1950 in response to the fast rise in the demand for electricity. Transformers with 800 kV and even higher kV ratings were made in the early 1980s, while ratings as high as 1100 MVA were produced in the early 1970s [2]. Transformers are basically divided into two classes according to their purpose of use: power transformers and distribution transformers. Power transformers are used in transmission networks of higher voltages for step-up and step-down applications (400 kV, 200 kV, 110 kV, 66 kV, 33 kV) and are generally rated above 200 MVA.

Traditionally, transformers that transform the voltage down to the domestic consumer voltage (usually 400 V or less) are called distribution transformers. IEC (International Electrotechnical Commission) standards do not distinguish between distribution transformers and power transformers. So both of these are transformers whose purpose is to convert power from one voltage level to another.

In general distribution transformers are used to reduce primary system voltages (2.4-34.5 kV) to utilization voltages (120-600 V). The distribution transformer is used for end-user connectivity (11 kV, 6.6 kV, 3.3 kV, 440 V, 230 V) and is generally rated less than 200 MVA. The distribution transformer is always online and operated at loads less than full load for most of the time. Hence, it is designed such that core losses are minimal.

The distribution transformer supplies medium and low voltage levels to residential, commercial, and industrial loads to adjust the voltage level to the final consumers [12]. The distribution transformer is the main power equipment at the end of the power system. Its dependable and safe operation has a direct impact on the power distribution system's operational state [13].

Due to their sizes and varieties, protection approaches of distribution transformers differ depending on the situation [14]. It is common practice to provide mechanical relays such as All transformers with a 0.5 MVA or higher are protected with Buchholz relays and sudden pressure relays. The purpose of mechanical relays is to identify malfunctions that the main relay is unable to identify. The primary safety feature on all small-size distribution transformers is HV fuses alone. Transformers up to 1000 kVA are frequently protected by fuses and MV circuit breakers. Restricted earth fault protection and over-current protection are used for all bigger rated and significant distribution transformers.

Transformers rated higher than 10 MVA ought to have differential protection. For transformers, current differential relays are used as primary protection. The two major methods used for backup protection are either distance protection overcurrent (phase current, zero sequence current) protection, or both. Thermal overload protection is frequently used in addition to these relays, but its primary purpose is to prolong the life of transformers rather than to identify defects. To safeguard the system, extra components including disconnectors, breakers, and surge arresters are installed externally on traditional distribution transformers.

High-performance distribution transformers are a well-known application of CSP technology [15]. It provides operation simplicity and reduces the maintenance and operational issues related to distribution transformers. With the use of surge arresters and CSP technology, a transformer can defend itself from LV side failures, overloads on the HV side, and lightning strikes. A signal light is used to visually alert the user of overload conditions. Additionally, CSP techniques protect the distribution system in which the transformer is connected [16].

In this thesis, a 500 kVA, 33/0.4 kV CSP distribution transformer will be designed and implemented. As a combination of existing CSP designs, protection will be provided both by the interrupter on the primary side and by the circuit breaker in the cable box to be located on the secondary side. Thus, there will be no need for an oil type circuit breaker. Protection systems will be located internally on this transformer. Thanks to the thermal protection system on it, it will also provide protection against long-term overloads. In the event of a fault, only the loads will be affected as the transformer will isolate itself from the distribution network to which it is connected. The signal lamp on it will provide information to the distribution system operator about the need to switch to greater power. Since surge arresters that will protect the transformer from lightning strikes are located on the transformer tank, they will provide more effective protection.

Distribution transformers can be divided into two groups according to their methods of cooling: (i) dry-type transformers and (ii) oil-immersed type transformers. Dry-type transformer cooling types are air natural (AN) cooling, air forced (AF) or air blast (AB) cooling. Oil-immersed transformer cooling types are oil natural air natural (ONAN) cooling, oil natural air forced (ONAF) cooling, oil forced air forced (OFAF) cooling, oil forced air natural (OFAN), oil natural water forced (ONWF), and oil forced water forced (OFWF) cooling.

Various studies have been published related to oil-immersed type transformers in literature. Main focuses of the publications are fault detection/diagnosis, testing methods [17], condition monitoring, prediction of thermal behaviour and aging [18, 19].

Condition monitoring is very crucial in oil-immersed type transformers in terms of fault detection and maintenance. Thanks to a fast and accurate monitoring technique, more effective and reliable operations can be achieved in these transformers. The mentioned techniques are examined in four basic categories as conventional interpretation methods, mathematical statistics methods, artificial intelligence-based methods and equivalent electric circuit simulation models.

In [20], conventional fault diagnosis techniques are reviewed in detail. These techniques are dissolved gas analysis, partial discharge, frequency response analysis, vibration analysis, hot spot temperature analysis, breakdown voltage, interfacial tension, transformer turn ratio, acidity, recovery voltage measurement, polarization current, insulation resistance, and degree of polymerization.

In [21], a mathematical grey clustering analysis method has been used for fault diagnosis in oil-immersed transformers. It has been stated that the proposed method is easy to implement in practice via a portable device. Additionally, it is seen as an advantage that it involves fewer processing steps compared to other artificial intelligence-based methods.

In [22], a gradient-boosting model optimized by the Bayesian-based method for detecting faults in oil-immersed transformers and reactors is described. The model outperforms other machine learning techniques and is superior to conventional methods. The software is developed for on-site fault detection and includes actual dissolved gas values from internal inspections. This study aims to improve fault diagnosis, prevent hazardous conditions, and reduce downtime costs for utilities.

A bi-level fault diagnosis method using XGBoost models is introduced in [23] to detect power transformer operation states. The first-level model reduces missing fault detection, while the second-level model accurately identifies different fault types. Custom functions and a hyperparameter tuning method improve diagnosis accuracy. An explainable method is used to derive fault feature selections, affecting each transformer operation state and sample. It has been stated that the two-level explainable method outperforms other machine-learning methods in power transformer diagnostics.

In [24], the effectiveness of low-cost piezoelectric sensors in detecting and monitoring partial discharges (PDs) in oil-filled transformers has been investigated. Two types of piezoelectric sensors were tested using time domain, frequency domain, and time-frequency analysis. The results showed that these sensors can effectively monitor PD in oil-filled transformers, distinguishing them from on-site noise and interference.

A hybrid model comprised of a genetic algorithm and support vector machine for moisture diagnosis in transformers has been developed in [25]. The model uses frequency-domain spectroscopy to obtain feature parameters. The model is tested in lab and field conditions to verify its feasibility and accuracy. The proposed model is seen as an intelligent moisture diagnostic tool in power transformers and thus it is emphasized that it has an important place in determining the service life of the transformer.

In [26], a method for detecting oil-immersed transformer faults by minimizing maintenance costs is elaborated. The method is straightforward and suitable for real-time online fault detection for oil-immersed type transformers. The method's performance is verified by its detection accuracy. It has been pointed out that the detection accuracy in fault diagnosis of oil-immersed type transformers is increased and maintenance costs are reduced through the proposed method.

Probabilistic neural network-based techniques with the dissolved gas analysis have been highlighted for fault detection in oil-immersed transformers in [27] and [28]. According to the simulation results, it has been pointed out that high accuracy values were achieved and the shortcomings of traditional dissolved gas analysis methods were eliminated. Moreover, a probabilistic method for the prediction of the allowable current of an oil-immersed type transformer is explained in [29].

On the other hand, researchers have recently introduced new methods for predicting the hot spot temperature (HST) of distribution transformers using electrical and mechanical properties. In [30], a detailed study related to condition monitoring of oil-immersed type transformers has been posited. In [31], an experimental study related to HST estimation was performed using optical fiber sensors. A novel method for monitoring the distributed temperature of insulation oil in a distribution transformer tank using optical fiber sensors is put forward in [32].

One of the key elements that influence the transformer oil-paper insulation deterioration is transformer winding HST. A 3-D electromagnetic-fluid-thermal analysis method for calculating transformer winding HST in a 10 kV oil-immersed distribution transformer is studied in [33]. Similarly, HST estimation was carried out for a 10 kV oil-immersed transformer in [34] with the support vector regression method. The feasibility and accuracy of the proposed calculation methods has been confirmed by simulation results and experimental results.

In [35], HST monitoring was carried out with current-voltage measurements in the windings for a single-phase oil-type transformer. The design of the oil-immersed transformer monitoring and integrated self-diagnosis system is pointed out in [36]. In [37], a thermal aging design has been addressed in order to gather information on the status of insulation through diagnostic tests and condition monitoring. In addition, internet of things based transformer monitoring systems are also available [38].

Transformers have a physical limitation in power transfer because of their nature. Typical features of this energy limit and how it can be calculated in oil-type transformers are described in [39]. In this way, it is aimed to prevent high temperature stress and at the same time maximize efficiency by operating the transformer at its energy limit.

Oil-immersed type transformers have been also encountered in different applications such as high voltage direct current (HVDC) wind farms [40] and lightning surge analysis [41]. In [40], a prototype of 50 kW oil-immersed transformer was handled. In [41], a circuit model of a 500 kV oil-immersed type transformer was created and lightning surge analysis was performed with this model.

Using the finite element method, the electromagnetic losses and heat transfer processes in a 3-phase oil-forced transformer are detailed in [42]. Leakage magnetic flux, eddy current loss densities, and the effect of electromagnetic loss in metal components on HST and oil flow were investigated. It is concluded that the surface current produced by the stray magnetic flux and the relative magnetic permeability of the metal components significantly affect the electromagnetic loss and core heat transfer. In another study, [43], temperature measurements and mechanical properties were examined using the finite element method in an oil-type transformer, and losses were calculated.

In [44], the response surface method is used to optimize an oil-immersed transformer cooling system. A 3-D computational fluid dynamic model is developed and followed by verification. According to simulation results, two response surface methods, the 2nd-order polynomial approach and the Kriging method, are evaluated. After that, the results have been compared to direct optimization approaches.

Traditionally, the transformer temperature is calculated by adding the oil temperature, winding temperature and ambient temperature rise. However, there is a difference between the HST calculated in this way and the measured temperature. The reason for this is that environmental factors have a late effect on the transformer. By making improvements in this regard in [45], the internal temperature of the transformer can be adjusted more accurately and a new HST calculation method has been developed.

3. MATERIALS AND METHODS

When CSP transformer examples around the world were examined, it was seen that protection was provided by two different methods. In the first widely used method, the primary part of the transformer is protected by an internal fuse and the secondary part is protected by an oil-type low voltage circuit breaker. In the second method used by companies such as ABB and Eaton, protection functions are performed on the primary side. Below is basic information about both designs.

As an example of the first widely used approach, a single-phase CSP transformer internal design prepared by an Indian company is given in Figure 3.1.

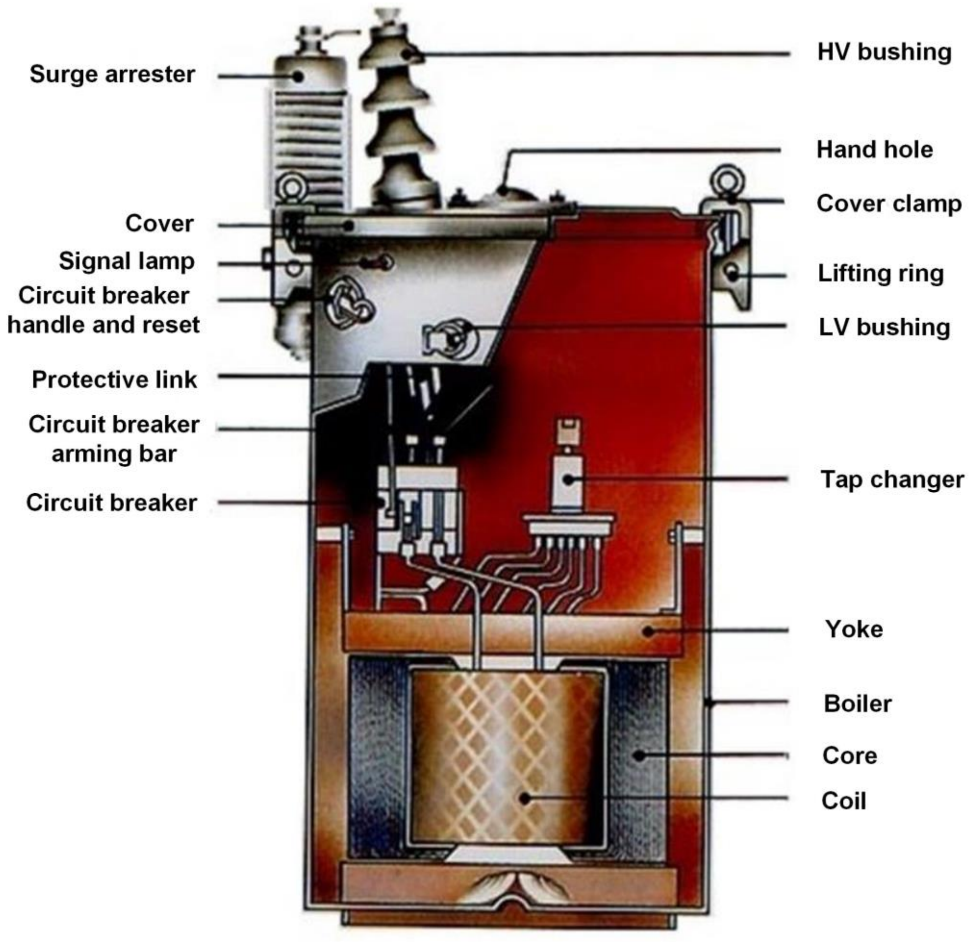

Figure 3.1. internal design view of CSP transformer.

As seen in Figure 3.1, there is all the necessary equipment on a CSP transformer to allow it to be used as plug and play. Surge arrester, fuse and circuit breaker constitute the basic parts of the CSP transformer.

A typical CSP transformer has ten main components. The following is a list of the main system components.

i. Transformer core: consist of specially laminated Silicon allow metal sheets
ii. Winding: cupper wires with isolation lamination
iii. Insulation: the insulating material of the transformer
iv. Tank: consist of active part of transformer and cooling oil
v. Bushings and other accessories: LV bushing, HV bushing, thermometer, oil-level indicator, protection relay etc.

vi. Dehydrating breather: the silica gel used in transformers with oil conservators keeps moisture inside, preventing deterioration of the air inside the oil conservator
vii. Oil conservator: includes additional oil to keep the transformer cool
viii. Buchholz Relay: transformers with oil conservator (oil reservoir) may have a gas detector relay (Buchholz relay) to detect air bubble or buildup of gas inside the transformer
ix. Tap changer: is a mechanism in transformers which adjusts turn ratios to be selected in discrete steps. Tap changers are often placed on the higher voltage winding side (lower current) for easy access and to minimize the current load during operation
x. Oil filling and oil drain valve: to fill and to drain oil into the transformer
xi. Lifting lugs: to lift transformer from safety place without damaging fins, active part and tank of transformer
xii. Earthing terminals: provide grounding of leakage electricity
xiii. Fins: provide cooling of transformer from excessive heat generation
xiv. Transformer oil: provide cooling of transformer from excessive heat generation

In traditional transformers, high-voltage fuses are located outside the transformer. Especially in pole-type transformers used in rural areas, fuses are exposed to rain and wind and blow due to mechanical stress. In CSP transformers, fuses are placed in series with the primary winding. Although it varies depending on the design, these fuses are generally placed inside the primary bushing. The part shown as the protective link in Figure 3.1 is actually the high-voltage fuse. The fuse is used to protect the distribution system from malfunctions that may occur within the transformer. A fault that may occur in or within the transformer windings will cause a high current and the fuse will melt and open the circuit, preventing the fault from reflecting on the distribution system. Figure 3.2 shows the protection ties (fuses) used in CSP transformers as an example.

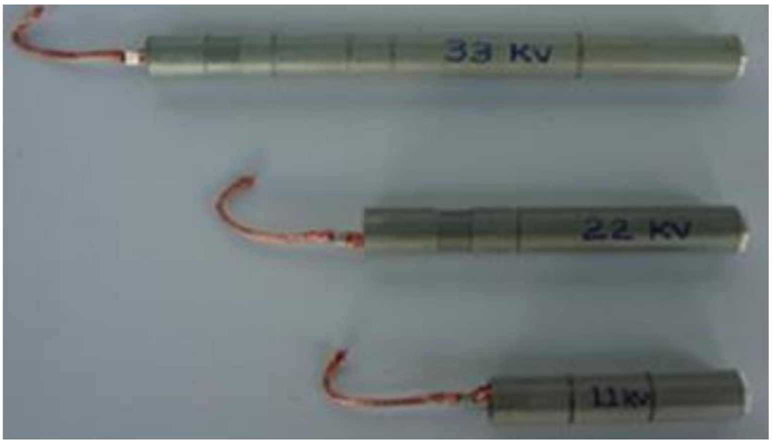

Figure 3.2. Protection ties for different voltage levels.

Another component that must be placed internally within the CSP transformer is the low-voltage circuit breaker. This circuit breaker is the basic element of CSP technology and provides overcurrent protection. This circuit breaker operates in transformer oil and performs its protection function thermally. The average temperature inside a transformer is equal to the sum of the average oil temperature and the average value of the winding heating. In order for the transformer not to age before expected, the average temperature value must not exceed certain limits. One of the main tasks of the circuit breaker is to prevent the average winding temperature from rising above a specified value. However, maximum oil temperature is another limiting factor. The circuit breaker to be used must also take this factor into consideration. Figure 3.3 gives an example of an oil-type circuit breaker that can be used in CSP transformers.

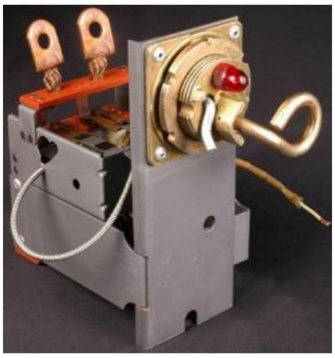

Figure 3.3. Example of oil type circuit breaker.

Another function of the CSP transformer circuit breaker is secondary fault protection. The breaker is quickly switched on to prevent any faults that may occur in the lines fed by the transformer from damaging the transformer. After the fault is eliminated with the help of a winding lever placed on the transformer, the circuit breaker can be brought to the active position again and the transformer can be put into operation.

Another feature of the CSP transformer is the signal lamp placed on the boiler. By means of this lamp, it can be monitored whether the transformer has reached an overload condition. When the transformer is forced to overload at any time, the lamp starts to burn. Another ability of the circuit breakers in CSP transformers is that they allow emergency operation. When the circuit breaker emergency operating method is turned off, the transformer will continue to operate although thermally stressed. In such an operating situation, the transformer may age rapidly.

On the other hand, one of the most critical points in CSP transformer design is the correct coordination of the input fuse and circuit breaker. Using the operating curves of the fuse and circuit breaker, the tripping of the circuit breaker must be coordinated before the input fuse blows. If this coordination is not done properly, the input fuse will trip without tripping the circuit breaker. Therefore, the circuit breaker will not be able to fulfill its protection function.

In the second method used in the production of CSP transformers, protection is provided on the primary side of the transformer. One of the companies using this method is ABB. Figure 3.4 shows the block diagram of CSP transformers developed by this company.

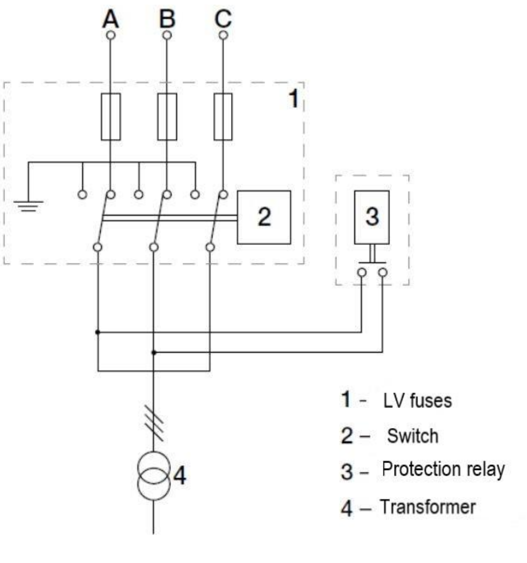

Figure 3.4. CSP transformer block diagram produced by ABB company.

In Figure 3.4, A, B and C represent high-voltage phase inputs. There are high-voltage fuses at the input ends of the boiler. After the fuses, an interrupter that acts as a high-voltage circuit load break switch is placed on the primary side. The protection device provides protection by constantly measuring the pressure and oil level in the boiler. After primary protection, windings are used for voltage conversion. Figure 3.5 gives an example of the line breaker preferred in these products.

Figure 3.5. Example of three-phase line interrupter.

The duty of the line breaker is to perform both protection and switch functions for the transformer. Secondary short circuits and overloads cause the breaker to trip. After the error is resolved, the breaker can be reinstalled.

The transformer to be developed in this thesis will have different designs than conventionally produced transformers. An improved design that is a combination of both the first method and the second method will be studied. These differences are listed below.

- The main protection function will be solved by adding an interrupter on the primary side, as in the second method.
- Another different feature of the CSP transformer is its internal fuse (protective link). The design will be made to ensure coordination between the circuit breaker and the fuse. In case of a fault, the circuit breaker is expected to open first. For this reason, coordination between fuse tripping curves and breaker tripping curves will be used.
- If the oil type circuit breaker is preferred, a winding lever is required to be used to activate the circuit breaker after it has been opened. This branch must be accessible to external distribution system operators. The winding lever is a movable component and one end of the lever must be connected to the circuit breaker in oil while the other end

must be accessible from the boiler. This point will be taken into consideration in the designs.

- Unlike the practices in the world, as a combination of the first and second methods, there will be thermal magnetic protections in a cable box to be placed on the transformer boiler for extra protection on the secondary side. As far as is known, this type of solution has not been presented before in practice or in the literature. Figure 3.6 shows the draft visual prepared for the CSP transformer, which is the output of this thesis.

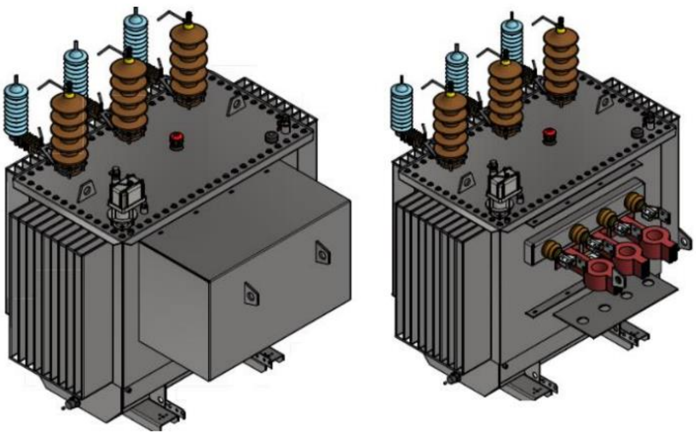

Figure 3.6. CSP transformer draft drawings (cable box closed on the left, open on the right).

There are many different stages in the design process of a transformer. After some calculations and drawings were carried out, products began to be created with endless calculations and parameter changes using computer-aided drawing and design software. Although the design is detailed theoretically in this thesis, parametric design is also used in practice. In parametric design, one of the algorithmic thinking approaches, the design is guided by a number of variables, parameters and rules. With the advancement of computer-aided design, parametric design has become a tool used in the creation of multi-layered products with smoother forms. Computer-aided design (CAD) programs such as ANSYS/Maxwell, CATIA and Autodesk Inventor can be used for parametric design of transformers.

Transformer design process is accomplished in mainly three steps;

- Electrical design
- Mechanical design
- Thermal design

Transformer design begins with designing the active part consisting of coil and core. After the dimensions of the active part of the transformer are decided, the dimensions of the tank parts are determined by taking into account the electrical jump distances, mechanical strength of the material, operating conditions and losses.

3.1. Electrical Design

In the electrical design of the transformer, we need some design parameters and calculated parameters listed below;

- Power rating of transformer
- Voltage levels (primary and secondary)
- Currents on both sides
- Primary and secondary coils wire diameter/size
- Net iron core area
- Numbers of turns (primary and secondary)

For an optimum design, the transformer should be designed to keep one of the following quantities as minimum as possible;

- Total volume
- Total weight
- Total cost
- Total loss

‘r’ ratio which is displayed in Equation 3.1, varies all of the previously listed values.

$$r = \phi_m / AT \tag{3.1}$$

A large cross-section is needed if we select a high value for "r," which will result in a higher iron loss as well as an increase in iron volume, weight, and cost. Additionally, the volume, weight, and cost of copper as well as copper losses fell as a result of the decline in the value of "AT." Therefore, "r" is a controlling factor for the quantities mentioned above. The core area is determined by the value of the flux density in the core, thus selecting the right one is crucial. A high flux density results in a reduced core area and lower iron costs. Additionally, a small core size results in a lower mean turn of winding, which lowers the cost of copper. However, increased flux density also increases iron losses, which raises temperature. The transformer's service circumstances also affect the flux density value. A distribution transformer designed to minimize iron losses and boost overall efficiency using a low flux density.

The active part of the transformer, which includes the core, primary and secondary windings, and bobbins, is seen in Figure 3.7. The cost and efficiency of a transformer design are two critical factors that must be taken into account. The transformer will be designed to its best potential if these parameters are supplied at the highest possible level. This section provides a detailed explanation of the mathematical model for a three-phase oil-type transformer. The following lists the fundamental equations, units, meanings, and symbols used in transformer computations. The relationship between the physical dimensions of machines and their electrical rating is provided by the output equation.

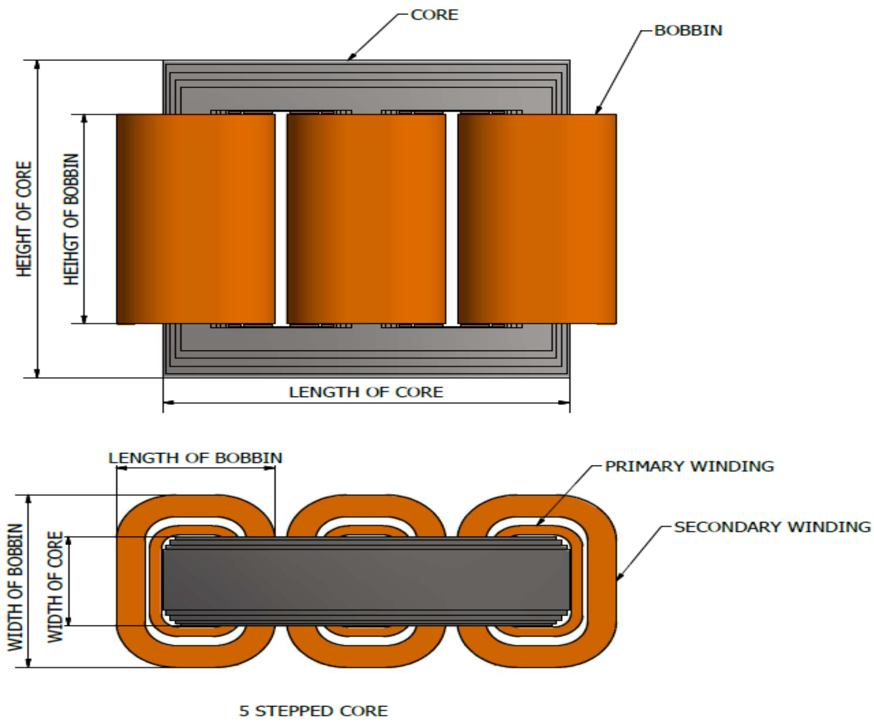

Figure 3.7. The transformer core and windings.

Here,

V_1 : primary or input voltage

V_2 : secondary or output voltage

I_1 : primary or input current

I_2 : secondary or output current

N_1 : primary number of turns

N_2 : secondary number of turns

a_1 : sectional area of low-voltage conductors (m^2)

a_2 : sectional area of high-voltage conductors (m^2)

δ : permissible current density (A/m^2)

Q : rating in kVA

f : frequency

Ø_m : maximum flux in the core

A_i = sectional area of core

B_m = maximum flux density in the core

The transformer rating for a 1-phase core type is provided by [10, 46, 47],

$$a_1 = I_1/\delta \quad (3.2)$$

$$a_2 = I_2/\delta \quad (3.3)$$

$$Q = V_1 * I_1 * 10^{-3}\text{kVA} \quad (3.4)$$

$$Q = (4.44 * f * \text{Ø}_m * N_1) * I_1 * 10^{-3}\text{kVA} \quad (3.5)$$

$$Q = (4.44 * f * (A_i * B_m) * N_1) * I_1 * 10^{-3} \text{ kVA} \quad (3.6)$$

$$K_w = \frac{\text{Actual Cu Section Area of Windings in Window}}{\text{Window Area } (A_w)} \quad (3.7)$$

$$K_w = \frac{(a_1 * N_1) + (a_2 * N_2)}{A_w} \tag{3.8}$$

$$K_w = \frac{\left(\left(\frac{I_1}{\delta}\right) * N_1\right) + ((I_2/\delta) * N_2)}{A_w} \; (\because a_1 = I_1/\delta \;\; \& \; a_2 = I_2/\delta) \tag{3.9}$$

$$K_w = \frac{(I_1 * N_1) + (I_2 * N_2)}{\delta * A_w} \tag{3.10}$$

$$K_w = \frac{2 * (I_1 * N_1)}{\delta * A_w} \tag{3.11}$$

For ideal transformer [46],

$$(I_1 * N_1 = I_2 * N_2) \tag{3.12}$$

So,

$$N_1 * I_1 = \frac{\delta * K_w * A_w}{2} \tag{3.13}$$

Put the value of $N_1 * I_1$ to convert equation 3.12 to equation 3.13,

$$Q = 4.44 * f * A_i * B_m * \left(\frac{\delta * K_w * A_w}{2}\right) * 10^{-3} \text{ kVA} \tag{3.14}$$

$$Q = 2.22 * f * A_i * B_m * \delta * K_w * A_w * 10^{-3} \text{kVA} \tag{3.15}$$

For single-phase shell type transformer, the window space factor can be found as,

$$K_w = \frac{(a_1 * N_1) + (a_2 * N_2)}{A_w} \tag{3.16}$$

$$K_w = \frac{((I_1/\delta) * N_1) + ((I_2/\delta) * N_2)}{A_w} \tag{3.17}$$

$$K_w = \frac{(I_1 * N_1) + (I_2 * N_2)}{\delta * A_w} \tag{3.18}$$

$$K_w = \frac{2*(I_1*N_1)}{\delta*A_w} \quad (3.19)$$

For ideal transformer [46],

$$(I_1 * N_1 = I_2 * N_2) \quad (3.20)$$

So,

$$N_1 * I_1 = \frac{\delta* K_w *A_w}{2} \quad (3.21)$$

Put the value of $N_1 * I_1$ to convert equation 3.20 to equation 3.5,

$$Q = 4.44 * f * A_i * B_m * (\frac{\delta* K_w *A_w}{2}) * 10^{-3}\text{kVA} \quad (3.22)$$

$$Q = 2.22 * f * A_i * B_m * \delta * K_w * A_w * 10^{-3}\text{kVA} \quad (3.23)$$

This equation is same for single-phase core type transformer. For three-phase core type transformer rating is given by,

$$Q = 3 * V_1 * I_1 * 10^{-3}\text{kVA} \quad (3.24)$$

$$Q = 3 * (4.44 * f * \emptyset_m * N_1) * I_1 * 10^{-3}\text{kVA} \quad (3.25)$$

$$Q = 3 * (4.44 * f * (A_i * B_m) * N_1) * I_1 * 10^{-3}\text{kVA} \quad (3.26)$$

Window space factor,

$$K_w = \frac{Actual\ Cu\ Section\ Area\ of\ Windings\ in\ Window}{Window\ Area\ (A_w)} \quad (3.27)$$

$$K_w = \frac{2*[(a_1*N_1)+(a_2*N_2)]}{A_w} \quad (3.28)$$

$$K_w = \frac{2*[((I_1/\delta)*N_1) +((I_2/\delta)*N_2)]}{A_w} \quad (3.29)$$

$$K_w = \frac{2*[(I_1*N_1)+(I_2*N_2)]}{\delta*A_w} \tag{3.30}$$

$$K_w = \frac{2*[2*(I_1*N_1)]}{\delta*A_w} \tag{3.31}$$

For ideal transformer [46],

$$I_1 * N_1 = I_2 * N_2 \tag{3.32}$$

So,

$$N_1 * I_1 = \frac{\delta* K_w *A_w}{4} \tag{3.33}$$

Put equation value of $N_1 * I_1$ form equation 3.33 to equation 3.6,

$$Q = 3 * 4.44 * f * A_i * B_m * (\frac{\delta* K_w *A_w}{4}) * 10^{-3}\text{kVA} \tag{3.34}$$

$$Q = 3.33 * f * A_i * B_m * \delta * K_w * A_w * 10^{-3}\text{kVA} \tag{3.35}$$

For three-phase shell type transformer, window space factor,

$$K_w = \frac{(a_1*N_1)+(a_2*N_2)}{A_w} \tag{3.36}$$

$$K_w = \frac{((I_1/\delta)*N_1)+((I_2/\delta)*N_2)}{A_w} (\because \quad a_1 = I_1/\delta \quad \& \quad a_2 = I_2/\delta) \tag{3.37}$$

$$K_w = \frac{(I_1*N_1)+(I_2*N_2)}{\delta*A_w} \tag{3.38}$$

$$K_w = \frac{2*(I_1*N_1)}{\delta*A_w} \tag{3.39}$$

For ideal transformer [46],

$$I_1 * N_1 = I_2 * N_2 \quad (3.40)$$

So,

$$N_1 * I_1 = \frac{\delta * K_w * A_w}{2} \quad (3.41)$$

Put equation value of $N_1 * I_1$ form equation (3.39) to equation (3.36)

$$Q = 3 * 4.44 * f * A_i * B_m * \left(\frac{\delta * K_w * A_w}{2}\right) * 10^{-3}\text{kVA} \quad (3.42)$$

$$Q = 6.66 * f * A_i * B_m * \delta * K_w * A_w * 10^{-3}\text{kVA} \quad (3.43)$$

The choice of magnetic loading (B_m) is carried out as follows;

- For normal Si-Steel (0.35 mm thickness, 1.5%—3.5% Si)-0.9 to1.1T
- For HRGO (Hot Rolled Grain Oriented Si Steel)- 1.2 to 1.4 T
- For CRGO (Cold Rolled Grain Oriented Si Steel, 0.14-0.28 mm thickness)-1.4 to 1.7 T.

The selection of electric loading (δ) is as follows;

This depends upon cooling method used. There are three basic types of cooling: natural, forced and water cooling.

i. Natural Cooling: 1.4-2.3 A/mm^2

AN-Air Natural cooling.

ON-Oil Natural cooling.

OFN-Oil Forced circulated with natural air cooling.

ii. Forced Cooling: 2.3-4.0 A/mm^2

AB-Air Blast cooling

OB-Oil Blast cooling

OFB-Oil Forced circulated with air blast cooling.

iii. Water Cooling: 4,5 -6.0 A/mm^2

OW-Oil immersed with circulated water cooling.

OFW-Oil Forced with circulated water cooling.

As it is known, EMF per turn calculations;

$$V_1 = 4.44 * f * \O_m * N_1 \quad (3.44)$$

So, EMF / turn;

$$E_t = \frac{V_1}{N_1} = 4.44 * f * \O_m \quad (3.45)$$

$$Q = V_1 * I_1 * 10^{-3}\text{kVA} \quad (3.46)$$

$$Q = (4.44 * f * \O_m * N_1) * I_1 * 10^{-3}\text{kVA} \quad (3.47)$$

$$Q = E_t * N_1 * I_1 * 10^{-3}\text{kVA} \quad (3.48)$$

Magnetic loading=$\O_m$ (3.49)

Electric loading=$N_1 * I_1$ (3.50)

$$Q = E_t * \frac{\O_m}{r} * 10^{-3}\text{kVA} \quad (3.51)$$

Or,

$$Q = E_t * \frac{E_t}{4.44 * f * r} * 10^{-3}\text{kVA using equation} \quad (3.52)$$

$$E_t^{\,2} = (4.44 * f * r * 10^{-3}) * Q \quad (3.53)$$

Or,

$$E_t = K_t\sqrt{Q}\text{Volts/Turn} \quad (3.54)$$

where,

$K_t = \sqrt{4.44 * f * r * 10^{-3}}$ is a constant and values are, $K_t = 0.6$ to 0.7 generally for three-phase core type power transformer.

$K_t = 0.45$ for three-phase core type distribution transformer

$K_t = 1.3$ for three-phase shall type transformer

$K_t = 0.75$ to 0.85 for single-phase core type transformer

$K_t = 1.0$ to 1.2 for single-phase shall type transformer

Estimation of core x-sectional area A_i is given as:

$$E_t = K_t\sqrt{Q} \quad (3.55)$$

$$E_t = 4.44 * f * \emptyset_m \quad (3.56)$$

$$E_t = 4.44 * f * A_i * B_m \quad (3.57)$$

So,

$$A_i = \frac{E_t}{4.44 * f * B_m} \quad (3.58)$$

The core can be following types,

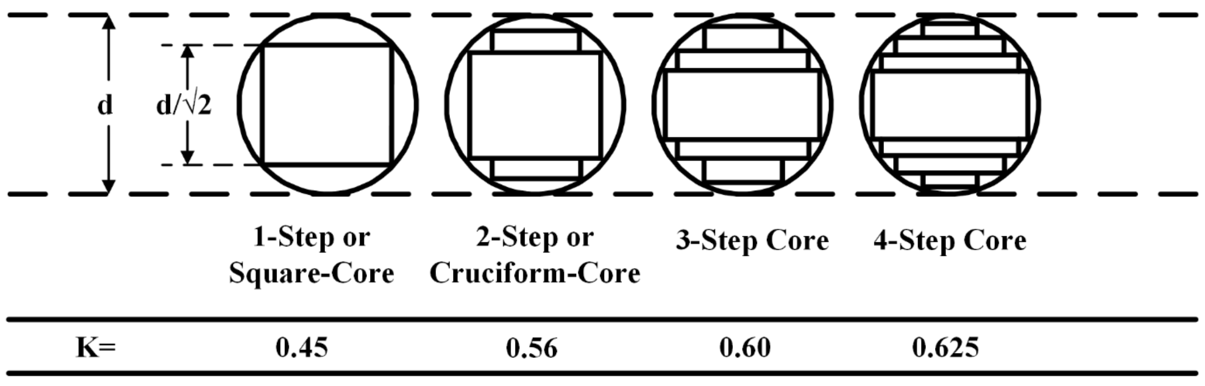

Figure 3.8. K factor depending on step number of core.

For square core,

$$\text{Gross Area} = \frac{d}{\sqrt{2}} * \frac{d}{\sqrt{2}} = 0.5 * d^2 \tag{3.59}$$

Let stacking factor, $K_i = 0.9$, then Actual Iron Area can be found;

$$A_i = 0.9 * 0.5d^2 \tag{3.60}$$

$$A_i = 0.45 * d^2 \tag{3.61}$$

Constant 0.45 value is for square core and take ‘’K’’ as a general case, so,

$$A_i = K * d^2 \tag{3.62}$$

Or,

$$d = \sqrt{\frac{A_i}{K}} \tag{3.63}$$

Graphical method can also be used to calculate the dimensions of the core. If we consider the two-step core shown in Figure 3.9.

$$\theta = \frac{90^\circ}{n+1} \tag{3.64}$$

n= number of steps, i.e. n =2.

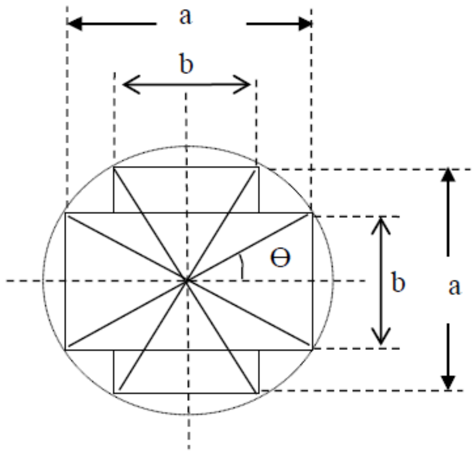

2-Step

Figure 3.9. Two-step core.

$$\theta = \frac{90^{\circ}}{2+1} = 30^{\circ} \quad (3.65)$$

So,

$$a = d * \cos\theta \quad (3.66)$$

$$b = d * \sin\theta \quad (3.67)$$

$$Percantage\ fill = \frac{Gross\ Area\ of\ Stepped\ core}{Area\ of\ circumcircle} = \frac{(K * d^2)/K_i}{\frac{\pi * d^2}{4}} \quad (3.68)$$

For four-step core of transformer,

$$percentage\ fill = \frac{(0.625 * d^2)/0.9}{\frac{\pi * d^2}{4}} 0.885\ \ or\ 88.5\% \quad (3.69)$$

Estimation of main dimensions;

$$Q = 3.33 * f * A_i * B_m * \ \delta * \ K_w \ * A_w * 10^{-3}\text{kVA} \quad (3.70)$$

So, window area,

$$A_w = \frac{Q}{3.33 * f * A_i * B_m * \delta * K_w * 10^{-3}} \ \ m^2 \quad (3.71)$$

Where,

$K_w =$ Window space factor for up to 10 kVA; (3.72)

$$K_w = \frac{8}{30 + HigherKV} \quad (3.73)$$

for up to 200 kVA;

$$K_w = \frac{10}{30+HigherKV} \quad (3.74)$$

for up to 1000 kVA;

$$K_w = \frac{12}{30+HigherKV} \quad (3.75)$$

For higher rating, $K_w = 0.15$ to 0.20 , assumed some suitable range for, $D =$ (1.7 to 2). Width of the window,

$$W_w = D - d \quad (3.76)$$

Height of the window,

$$L = \frac{A_w}{width\ of\ window(W_w)} \quad (3.77)$$

Generally, $\frac{L}{W_w} = 2\ to\ 4$, Yoke area A_y is generally taken 10% to 15% higher then core section area (A_i) to reduce the iron loss in the yoke section. But if we increase the core section area (A_i) more copper will be needed in the windings and so more cost through we are reducing the iron loss in the core. Further length of the winding will increase resulting higher resistance so cause higher core loss.

$$A_y = (1.1 \text{ to } 1.15) * A_i \quad (3.78)$$

Depth of yoke,

$$D_y = a \quad (3.79)$$

Height of the yoke,

$$h_y = \frac{A_y}{D_y} \quad (3.80)$$

Width of the core,

$$W = (2 * D) + d \quad (3.81)$$

Height of the core,

$$h = L + \left(2 * h_y\right) \quad (3.82)$$

Flux density in yoke [46],

$$B_y = \frac{A_i}{A_y} * B_m \quad (3.83)$$

Estimation of core loss and core loss component of no-load current I_c,

$$\text{Volume of iron in core} = 3 * L * A_i m^2 \quad (3.84)$$

$$\text{Weight of iron in core} = density * volume \quad (3.85)$$

$$\text{Weight of iron in core} = \rho_i * 3 * L * A_i \text{Kg} \quad (3.86)$$

$$\rho_i = density\ of\ iron\ (\frac{kg}{m^3}) \quad (3.87)$$

For normal iron/steel ,

$$\rho_i = 7600\ (\frac{kg}{m^3}) \quad (3.88)$$

For M-4 steel,

$\rho_i = 6500\ (\frac{kg}{m^3})$ (3.89)

From the graph we can find out specific iron loss, $p_i(\frac{Watt}{Kg})$ corresponding to flux density B_m in core. So,

Iron loss in core $= p_i * \rho_i * 3 * L * A_i$ Watt (3.90)

Similarly,

Iron loss in yoke $= p_y * \rho_i * 2 * W * A_y$ Watt (3.91)

Where,

$p_y =$ specific iron loss corresponding to flux density B_y in yoke

Total iron loss,

$p_i =$ Iron loss in core + Iron loss in yoke (3.92)

Core loss component of no-load current,

$I_c = \frac{Core\ loss\ per\ phase}{Primary\ Voltage}$ (3.93)

$I_c = \frac{P_i}{3V_1}$ (3.94)

Estimation of magnetizing current of no-load current I_m,

$(B_m \rightarrow \frac{at_{core}}{m} \qquad B_c \rightarrow \frac{at_{yoke}}{m})$

So,

$MMF\ required\ for\ the\ core = 3 * L * at_{core}$ (3.95)

$MMF\ required\ for\ the\ yoke = 2 * W * at_{yoke}$ (3.96)

We account 5% at for joints etc. So,

$$total\ MMF\ required = 1.05[MMF\ for\ core + MMF\ for\ yoke] \tag{3.97}$$

Peak value of the magnetizing current,

$$I_{m,peak} \rightarrow \frac{Total\ MMF\ required}{3N_1} \tag{3.98}$$

RMS value of the magnetizing current,

$$I_{m,RMS} \rightarrow \frac{I_{m,peak}}{\sqrt{2}} \tag{3.99}$$

$$I_{m,RMS} \rightarrow \frac{Total\ MMF\ required}{3\sqrt{2}N_1} \tag{3.100}$$

Estimation of no load current, if no load current is I_0,

$$I_0 = \sqrt{{I_c}^2 + {I_m}^2} \tag{3.101}$$

No load power factor,

$$\text{Cos}\,\emptyset_0 = \frac{I_c}{I_0} \tag{3.102}$$

The no-load current should not exceed 5% of the full load current.

Estimation of number of turns on LV and HV winding;

Primary no of turns,

$$N_1 = \frac{V_1}{E_1} \tag{3.103}$$

Secondary no of turns,

$$N_2 = \frac{V_2}{E_2} \tag{3.104}$$

Estimation of sectional area of primary and secondary windings;

Primary current,

$$I_1 = \frac{Q\times10^{-3}}{3V_1} \tag{3.105}$$

Secondary current,

$$I_2 = \frac{Q\times10^{-3}}{3V_2} \tag{3.106}$$

or,

$$I_2 = \frac{N_1}{N_2} I_1 \tag{3.107}$$

Sectional area of primary windings,

$$a_1 = \frac{I_1}{\delta} \tag{3.108}$$

Sectional area of secondary windings,

$$a_2 = \frac{I_2}{\delta} \tag{3.109}$$

Where δ is the current density.

Determination of R_1 & R_2 and CU losses;

Let, L_{mt} = Length of mean turn

Resistance of primary winding,

$R_{1,dc,75}=0.021 \times 10^{-6} \frac{L_{mt} N_1 (m)}{a_1 (m^2)}$ (3.110)

$R_{1,ac,75}=(1.15 \text{to} 1.20) R_{1,dc,75}$ (3.111)

Resistance of secodary winding,

$R_{2,dc,75}=0.021 \times 10^{-6} \frac{L_{mt} N_2 (m)}{a_2 (m^2)}$ (3.112)

$R_{2,ac,75}=(1.15 \text{ to } 1.20)\ R_{2,dc,75}$ (3.113)

Copper loss in primary winding=$3I_1^2 R_1$Watt (3.114)

Copper loss in secondary winding =$3I_1^2 R_2$Watt (3.115)

Total copper loss = $3I_1^2 R_1 + 3I_1^2 R_2 = 3I_1^2 (R_1 + R_2) = 3I_1^2 R_P$ (3.116)

$R_{01}=R_P=R_1 + R_2$ (3.117)

Total resistance referred to primary side. On no load, there is magnetic field around connecting leads etc. which causes additional stray losses in the transformer tanks and other metallic parts. There losses may be taken as 7% to 10% total cu losses.

Determination of efficiency [48];

Efficiency,

$$\mu = \frac{\text{Output Power}}{\text{Input Power}} \quad (3.118)$$

$$\mu = \frac{\text{Output Power}}{\text{Input Power+Losses}} \quad (3.119)$$

$$\mu = \frac{\text{Output Power}}{\text{Input Power+Iron Loss+Cu Loss}} \times 100\% \quad (3.120)$$

Estimation of leakage reactance;

Assumptions,

1. Consider permeability of iron as infinity that is MMF is needed only for leakage flux path in the window.
2. The leakage flux lines are parallel to the axis of the core.

MMF at distance x,

$$M_X = \frac{N_1 I_1}{b_1} x \tag{3.121}$$

Permeance of this elementary cylinder,

$$\mu_0 \frac{A}{L} = \mu_0 \frac{L_{mt} dx}{L_c}, \left(\therefore S = \frac{1}{\mu_0}\frac{L}{A} \quad \& \; Permeance = \frac{1}{S}\right) \tag{3.122}$$

L_c = Length of winding;

Leakage flux lines associated with elementary cylinder,

$$d\emptyset_x = M_x \times Permeance \tag{3.123}$$

$$\frac{N_1 I_1}{b_1} x \times \mu_0 \frac{L_{mt} d_x}{L_C} \tag{3.124}$$

Flux linkage due to this leakage flux [46],

$$d\Psi_x = \frac{N_1 I_1}{b_1} x \times \mathrm{d}\emptyset_x \tag{3.125}$$

$$d\Psi_x = \frac{N_1 I_1}{b_1} x \times \left(\frac{N_1 I_1}{b_1} x \times \mu_0 \frac{L_{mt} dx}{L_c}\right) \tag{3.126}$$

$$d\Psi_x = \mu_0 N_1^2 \frac{L_{mt}}{L_C} I_1 \left(\frac{x}{b_1}\right)^2 d_x \tag{3.127}$$

Flux linkages (or associated) with primary winding,

$$\Psi_1{}' = \mu_0 N_1^2 \frac{L_{mt}}{L_C} I_1 \int_0^{b_1} \left(\frac{x}{b_1}\right)^2 d_x = \mu_0 N_1^2 \frac{L_{mt}}{L_C} I_1 \left(\frac{b_1}{3}\right) \quad (3.128)$$

Flux linkages with the space ‘a’ between primary and secondary windings,

$$\Psi_0 = \mu_0 N_1^2 \frac{L_{mt}}{L_C} I_1 a \quad (3.129)$$

We consider half of this flux linkage with primary and rest half with the secondary winding. So total flux linkages with primary winding,

$$\Psi_1 = \Psi_1' + \frac{\Psi_0}{2} \quad (3.130)$$

$$\Psi_1 = \mu_0 N_1^2 \frac{L_{mt}}{L_C} I_1 \left(\frac{b_1}{3} + \frac{a}{2}\right) \quad (3.131)$$

Similarly, total flux linkages with secondary winding [46],

$$\Psi_2 = \Psi_2' + \frac{\Psi_0}{2} \quad (3.132)$$

$$\Psi_2 = \mu_0 N_2^2 \frac{L_{mt}}{L_C} I_1 \left(\frac{b_2}{3} + \frac{a}{2}\right) \quad (3.133)$$

Primary and secondary leakage inductance,

$$L_1 = \frac{\Psi_1}{I_1} = \mu_0 N_1^2 \frac{L_{mt}}{L_C} \left(\frac{b_1}{3} + \frac{a}{2}\right) \quad (3.134)$$

$$L_2 = \frac{\Psi_2}{I_2} = \mu_0 N_2^2 \frac{L_{mt}}{L_C} \left(\frac{b_2}{3} + \frac{a}{2}\right) \quad (3.135)$$

Primary and secondary leakage reactance,

$$X_1 = 2\prod f L_1 = 2\prod f \mu_0 N_1^2 \frac{L_{mt}}{L_C} \left(\frac{b_1}{3} + \frac{a}{2}\right) \quad (3.136)$$

$$X_2 = 2\prod f L_2 = 2\prod f \mu_0 N_2^2 \frac{L_{mt}}{L_C}\left(\frac{b_2}{3} + \frac{a}{2}\right) \quad (3.137)$$

Total leakage reactance referred to primary side,

$$X_{01} = X_p = X_1 + X_2' = 2\prod f \mu_0 N_1^2 \frac{L_{mt}}{L_C}\left(\frac{b_1+b_2}{3} + a\right) \quad (3.138)$$

Total leakage reactance referred to secondary side,

$$X_{02} = X_s = X_{1+}' X_2 = 2\prod f \mu_0 N_2^2 \frac{L_{mt}}{L_C}\left(\frac{b_1+b_2}{3} + a\right) \quad (3.139)$$

It must be 5% to 8% or maximum 10%. To control X_P, window height is changed. If increasing the window height (L), L_C will increase and following will decrease b_1 , b_2 and L_{mt} and so we can reduce the value of X_P.

Calculation of voltage regulation of transformer [46]:

$$V.R = \frac{I_2 R_{02}\cos\emptyset_2 \pm I_2 X_{02}\sin\emptyset_2}{E_2} \times 100 \quad (3.140)$$

$$V.R = \frac{R_{02}\cos\emptyset_2}{E_2/I_2} \times 100 \pm \frac{X_{02}\sin\emptyset_2}{E_2/I_2} \times 100 \quad (3.141)$$

$$V.R = \%R_{02}\cos\emptyset_2 \pm \%X_{02}\sin\emptyset_2 \quad (3.142)$$

The electrical design of the CSP transformer is obtained through certain parameters using a design program created based on the formulas given above. A visual representation of the design program is shown in Figure 3.10.

Nominal rating (kVA)	Top oil temperature rise	Winding temperature rise		Voltage LV	415 V
500 kVA	55 K	60 K		Voltage HV	33000 V
Frequency	Ambient temperature			testvoltage LV	3 kV
50Hz	45 ºC			testvoltage HV	70 kV
Connection symbol	Installed height			impulse voltage LV	_
Dyn11	<1000 m			impulse voltage HV	170 kV
Insulation class LV	Insulation class HV				
1,1 kV	36 kV				
Regulation					
Low Voltage (cu)		High Voltage (cu)			Radial Built
Phase current LV (A)	695,6	Phase current HV	5,1		Outside the windc
Foil Height (mm)	260,0	HV Height	224	Core diameter	150
		Wire Height (mm)	1,65	Obround part	142
Foil Thickness (mm)	1,1	Wire Thickness (mm)	1,65	Distance core/LV	3,0
Foil Section (mm^2)	286	Wire section (mm^2)	2 x 1 x 1	Inner diameter LV	156,0
		Wire insulation (mm)	0,090	Radial thickness LV	26,0
Inter Layer Insulation (mm)	0,14	Inter Layer Insulation (mm)	0,325	Outer diameter LV	208,0
Number of Turns LV	18	Number of turns HV	2705	Distance LV/HV	12,0
		Number of layers	23	Inner diameter HV	232,0
		Turns per layer	119	Radial Thickness HV	48,5
				Outer diameter HV - without ob.	

Figure 3.10. A visual representation of the design program.

The dimensions of the core obtained as a result of the electrical design performed according to the design parameters are illustrated in Figure 3.11.

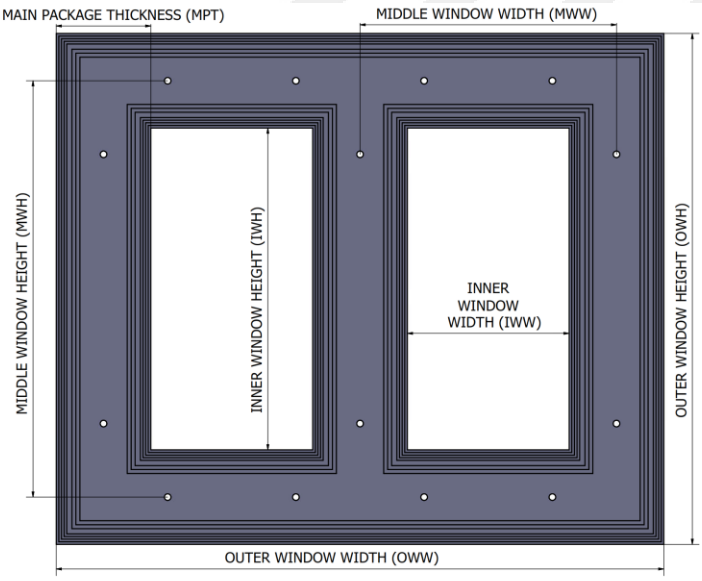

CORE DIMENSIONS	
MAIN PACKAGE THICKNESS	120 mm
MIDDLE WINDOW WIDTH	388 mm
MIDDLE WINDOW HEIGHT	490 mm
INNER WINDOW WIDTH	198 mm
INNER WINDOW HEIGHT	300 mm
OUTER WINDOW WIDTH	966 mm
OUTER WINDOW HEIGHT	680 mm

Figure 3.11. The dimensions of the core.

The core perspective view is shown in Figure 3.12 The 3*2 lateral lamination method have been used in the core design, and the magnetic field strength and the net useful cross section have been determined as 1,522 Wb/m^2 (T) and 435,02 cm^2, respectively. 0.27 mm thick CRGO sheet has been used in the core design, and the voltage per turn has been calculated as 14,77 V. The core loss is estimated to be 997 Watts.

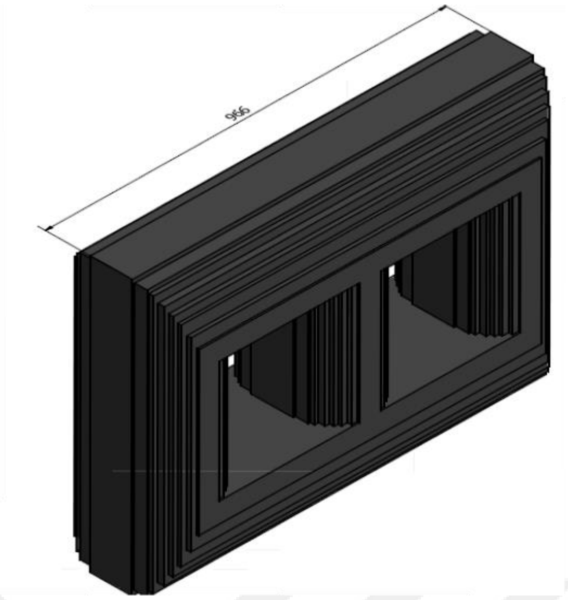

Figure 3.12. The core perspective view.

Because the low-voltage current of the transformer is 666.69 A, the current of the thermal magnetic switch used for circuit breaking is determined as an upper value (800 A). The Entes MPR-26S-21 model was used as the power analyzer. Insulation materials have Class A insulation. Using the Hermetic Protection Relay and Pressure Safety Valve, the transformer is protected against possible increases in pressure and temperature.

The winding dimensions were determined in accordance with the calculations performed for the high-voltage conductor and insulation materials, considering the determined core dimensions. The winding dimensions are shown in Figures 3.13 and 3.14. The overloading curve is demonstrated in Figure 3.11.

In the design of the insulation structure; a resin-impregnated insulation material called DDP is used to increase the mechanical strength of LV and HV windings. Insulation papers with insulating properties and oil channel strips are placed in the windings, creating an insulating environment. At the same time, the studs used in the active part are covered with an insulation material called crepe pipe; Thanks to the isolated environment created, electrical discharges are prevented. Special compression materials called green bandages are used to compress the core packages. Corner insulation materials are used to prevent damage to the coil at the corner turns between the core and the coil.

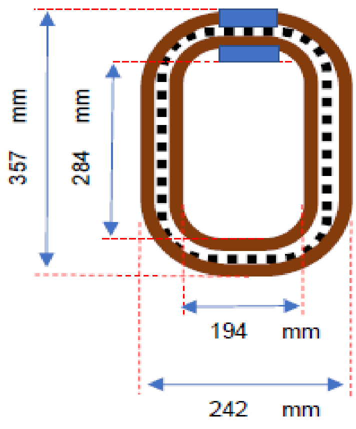

Figure 3.13. Low-voltage winding dimensions.

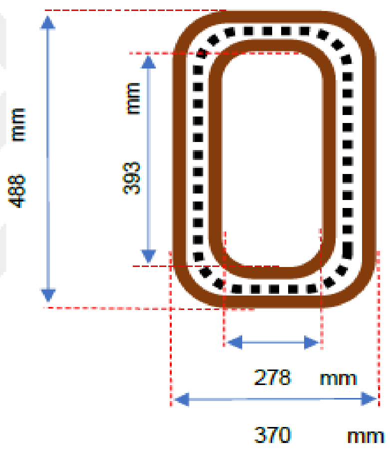

Figure 3.14. High-voltage winding dimensions.

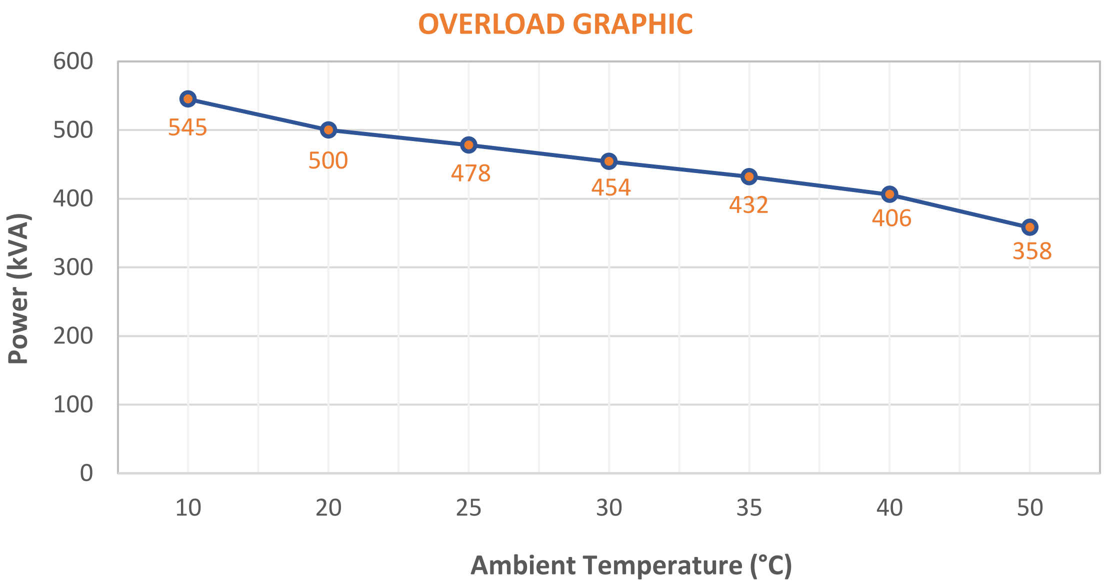

Figure 3.15. Overload curve according to ambient temperature (according to IEC 60076-7).

A short-circuit analysis of the electrically designed CSP transformer was performed, and the calculation of short-circuit impedances is presented in Table 3.1.

Table 3.1. Short Circuit Calculation

Tap	S_N (MVA)	U_1/U_2 (kV)			Uk (%)	Z_{TR-HV} (Ω/ph.)	Z_{TR-LV} (Ω/ph.)	Krest Factor
1	0,5	33	/	476,3	5,15	112,1670	0,0234	2,3050
3			/	433	5,09	110,8602	0,0191	2,2912
5			/	389,7	5,01	109,1178	0,0152	2,2748

3.2. Mechanical Design

Due to the losses in the transformer core and coil, the mechanical design of the tank with tubes is crucial. The core and coil's temperature rise is what causes these losses. The surrounding air in small-capacity transformers will efficiently cool the transformer and maintain the temperature rise well within allowable bounds. The losses and temperature rise in tandem with the transformer's increased capacity. Air blowing over the transformer might be necessary to maintain the temperature rising between limits. This is not recommended since the insulation may be impacted by the moisture, oil particles, and other contaminants in the surrounding air. In order to mitigate air dangers, the transformer is housed inside an oil-filled steel tank. Heat is transferred from the coil and core to the tank walls through the oil. Radiation and convection caused the heat to escape from the tank walls and into the surrounding atmosphere.

The transformer's cooling and insulation are crucial because of its place in the power system. The transformer and insulation system are subjected to electrical and thermal pressures that could destroy the insulation system entirely. One of the most frequent reasons for transformer failure is insulation failure. As a result, it is crucial to appropriately proportion the insulation system while designing transformers. It is crucial to consider throughout the dimensioning process that the electric field should not be more than the designated critical value and that the tank's design must be able to withstand the elevated temperature brought on by the magnetic field. This necessitates the employment of intricate analytical or numerical techniques for cooling system design throughout the design phase and electric field computation.

The coolant used to reduce excess heat in transformers is air and oil. Cooling techniques of transformers are illustrated in Table 3.1. The determining of the cooling technique depends upon the size, type of application and the type of conditions on installation sites. The symbols designated for these approaches depend upon the medium of cooling used and the type of circulation employed.

According to the medium, Air-A, Gas-G, Oil-O, Water-W, Solid insulation, according to the circulation type, Natural-N, Forced-F, according to the cooling type, Air Natural (AN), Air Blast (EU), Oil Natural They are classified as (ON), Oil Natural Air Forced (ONAF), Oil Natural Air Natural (ONAN), Oil Natural Water Forced (ONWF), Forced Circulation of Oil (OF).

Table 3.2. Cooling types of transformers

1.LETTER	2.LETTER	3.LETTER	4.LETTER

It relates to the cooling medium contact with the windings						It relates to the cooling medium contact with the external cooling system					
Types of cooling medium		Circulation type		Types of cooling medium		Circulation type		Types of cooling medium		Circulation type	
O	N	A	N	O	N	A	F	O	F	W	F
↓	↓	↓	↓	↓	↓	↓	↓	↓	↓	↓	↓
Oil	Natural	Air	Natural	Oil	Natural	Air	Forced	Oil	Forced	Water	Forced

3.2.1. Design of the transformer tank

The width of the transformer tank is computed by;

$$W_t = 2D + D_e + 2b \quad (3.143)$$

where,

$D_e = External\ diameter\ of\ HV\ winding$

$b = Clearance\ width\ wise\ between\ HV\ and\ tank$

The depth of transformer tank,

$$l_t = D_e + 2a \quad (3.144)$$

where,

$a = Clearance\ depth\ wise\ between\ HV\ and\ tank$

The height of transformer tank,

$$H_t = H + h \quad (3.145)$$

where,

$$h = h_1 + h_2 = Clearance\ height\ wise\ of\ top\ and\ bottom \quad (3.146)$$

3.2.2. Calculation of temperature rise

The surface area of four vertical sides of the tank (Heat is thought to disperse from the tank's four vertical sides, which together comprise its surface area):

$$S_t = 2(W_t + l_t)H_t \ m^2 \text{ (Excluding area of top and bottom of tank)} \quad (3.147)$$

Let $\theta = Temp\ rise\ of\ oil$ (35°C to 50°C) ;

$$Total\ full\ load\ losses\ (\ Iron\ loss\ +\ Cu\ loss) = 12{,}5 * S_t * \theta \quad (3.148)$$

So temp rise in °C ,

$$\theta = \frac{Total\ full\ load\ losses}{12{,}5 * S_t} \quad (3.149)$$

If the computed temperature rises beyond the threshold, an appropriate quantity of cooling tubes or radiators needs to be supplied.

3.2.3. Calculation of number of cooling tubes

Let,

$$Surface\ area\ of\ all\ cooling\ tubes \quad = x * S_t \quad (3.150)$$

Specific heat dissipation, $6 \frac{\text{Watt}}{m^2}$°C by radiation and $6{,}5 \frac{\text{Watt}}{m^2}$°C by convection. Afterwards, the transformer walls and cooling tubes must dissipate the total losses [46];

$$Total\ losses = (12{,}5 * S_t + 8{,}5 * x * S_t) * \theta \quad (3.151)$$

$$6W \text{ Radiation} + 6{,}5\text{W} = 12{,}5 \text{ Convection} \quad (3.152)$$

$$6{,}5 * 1{,}5W \approx 8{,}5\ (\approx 35\%\ more)\ Convection\ only \quad (3.153)$$

Thus, we can determine the total surface area of cooling tubes using the equation above.

total surface area of cooling tubes=$x * S_t$ (3.154)

In a transformer, 6 mm diameter tubes are often used, spaced at least 45 mm apart.

$$A_t = Surface\ area\ of\ one\ cooling = \pi * d_{tube} * l_{tube,mean} \quad (3.155)$$

Hence,

$$No\ of\ cooling\ tubes = \frac{x*S_t}{A_t} \quad (3.156)$$

The fin height, length, and spacing parameters have the greatest effects on the transformer's thermal performance. Additionally, the hotspot temperature is lowered by lengthening and raising the fins, however, the hotspot temperature is positively correlated with reducing fin spacing, which increases the surface for heat transfer. Also, it has been determined that fin height has a greater effect on the hot spot temperature than fin length and spacing. This has a significant impact on the transformer's lifespan and safer operation, resulting in improved performance and a significant increase in the transformer's lifetime.

3.2.4. Weight of the transformer

Let,

$$W_i = \text{Weight of Iron in core and yoke(core volume} * \text{density} + \text{yoke volume} * \text{density)Kg} \quad (3.157)$$

$$W_c = Weight\ of\ copper\ in\ winding(volume * density)\text{Kg}$$

$$(density\ of\ cu = 8900\frac{kg}{m^3}) \tag{3.158}$$

$$Weight\ of\ oil = Volume\ of\ oil * 880\text{Kg} \tag{3.159}$$

Add 20% of (W_i + W_i) for fittings, tank etc., total weight is equal to weight of above all parts [46].

The calculated weights of boiler, cover, active part and the oil are given in Table 3.3. The center of gravity visual is presented in Figure 3.16.

Table 3.3. Weight calculations

Component	**Weights (Kgs)**
Boiler	375
Cover	100
Active Part	1370
Oil	580
Total	2290

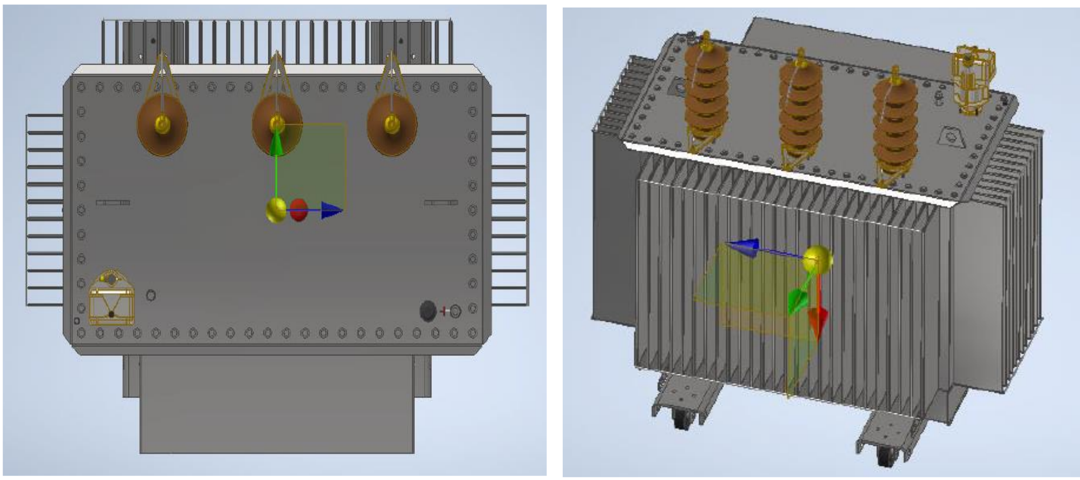

Figure 3.16. The center of gravity in the designed CSP transformer

The LV and HV bushing phase gaps are calculated based on the electrical jump distance, and the hole diameters are opened according to bushing type. Accessory placement is performed according to the optimum distance and ease of installation. A view of the cover perspective is presented in Figure 3.17.

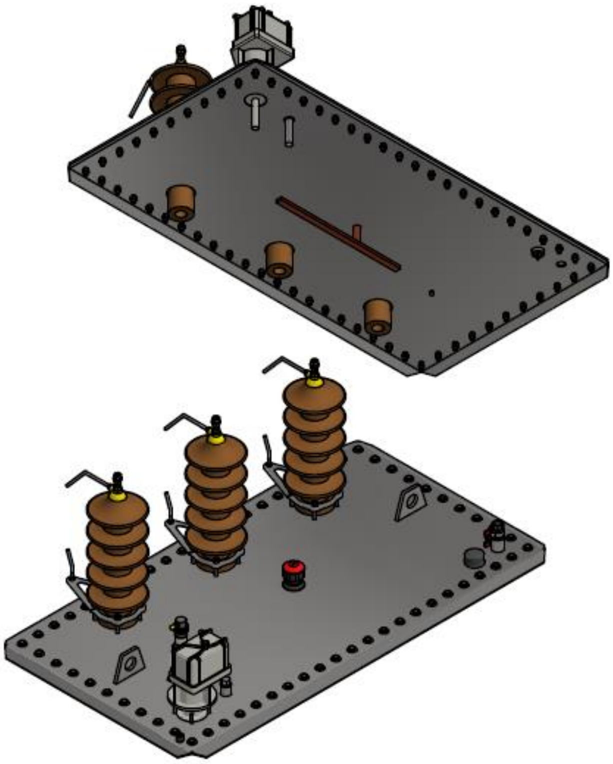

Figure 3.17. Cover of the CSP transformer (perspective view)

The frame hole diameter and the distance between the holes are given based on certain standards, according to the power of the transformer and the internal boiler distances, to provide the pressure that will prevent oil leakage between the transformer cover and boiler. Figure 3.18 displays the technical drawing of the frame. A view of the frame perspective is presented in Figure 3.19.

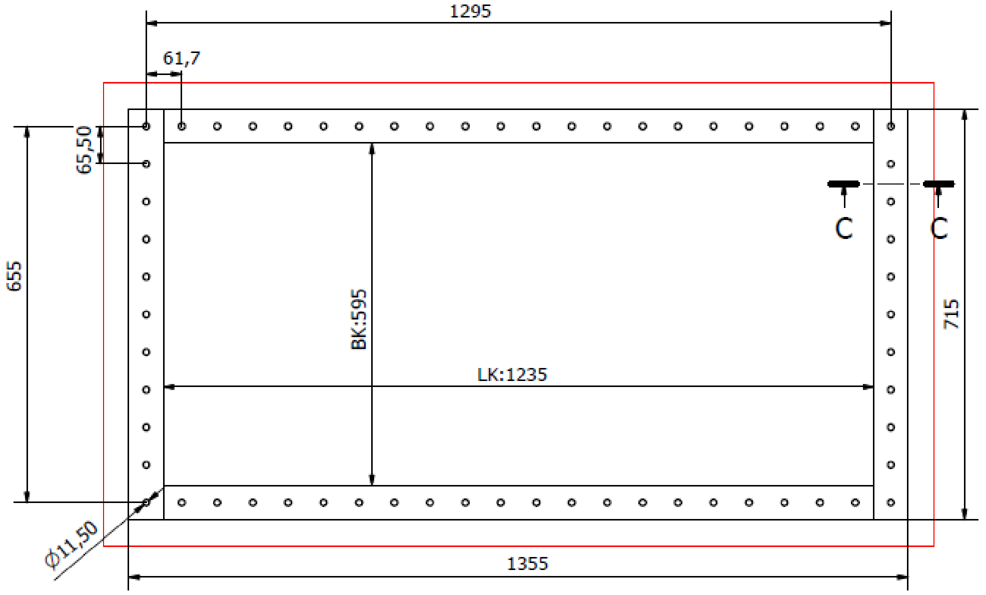

Figure 3.18. Technical drawing of the frame

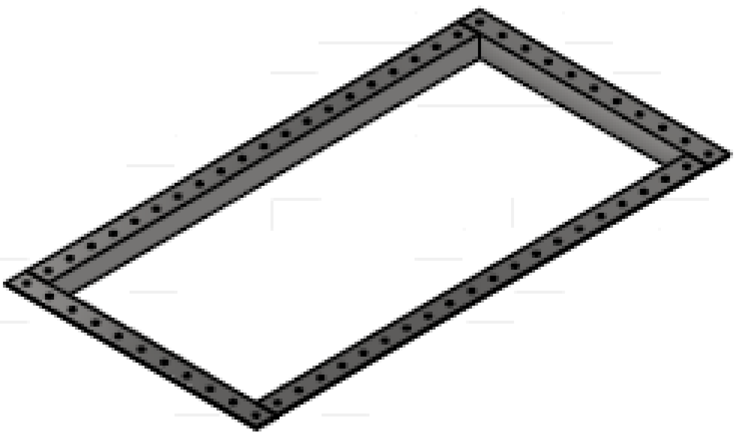

Figure 3.19. Frame (perspective view)

The technical drawing of the boiler is shown in Figure 3.20. The perspective view of the boiler can be seen from Figure 3.21. The assembled 3D images of the boiler, frame and cover are presented in Figure 3.22. The active part of the transformer is demonstrated in Figure 3.23.

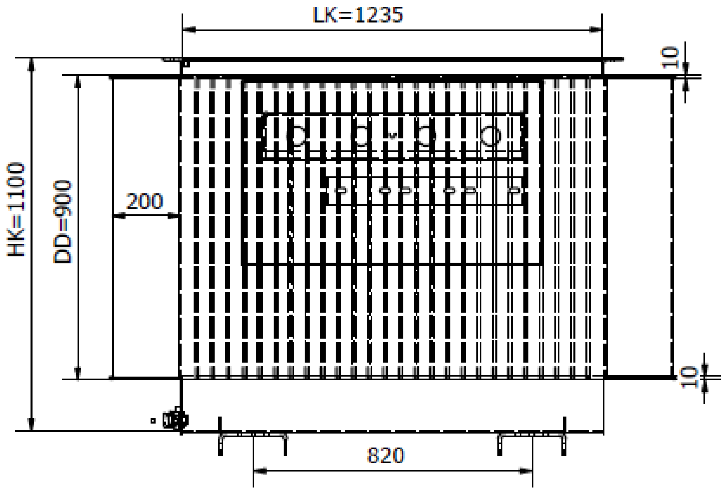

Figure 3.20. Technical drawing of the boiler

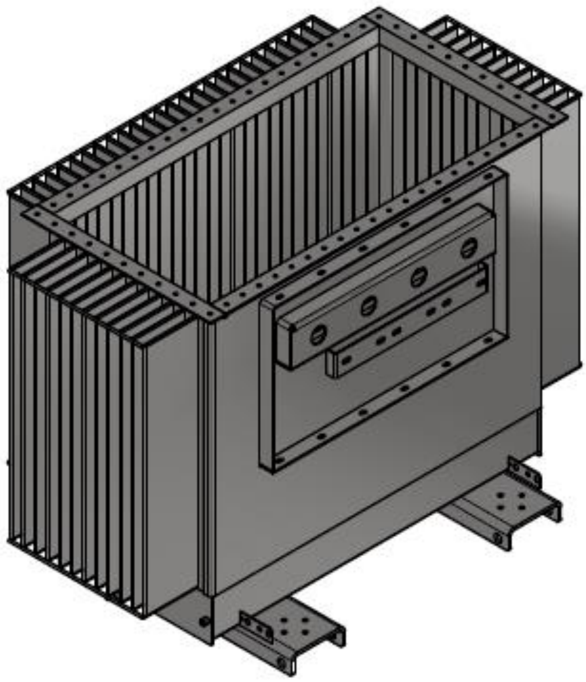

Figure 3.21. Boiler (perspective view)

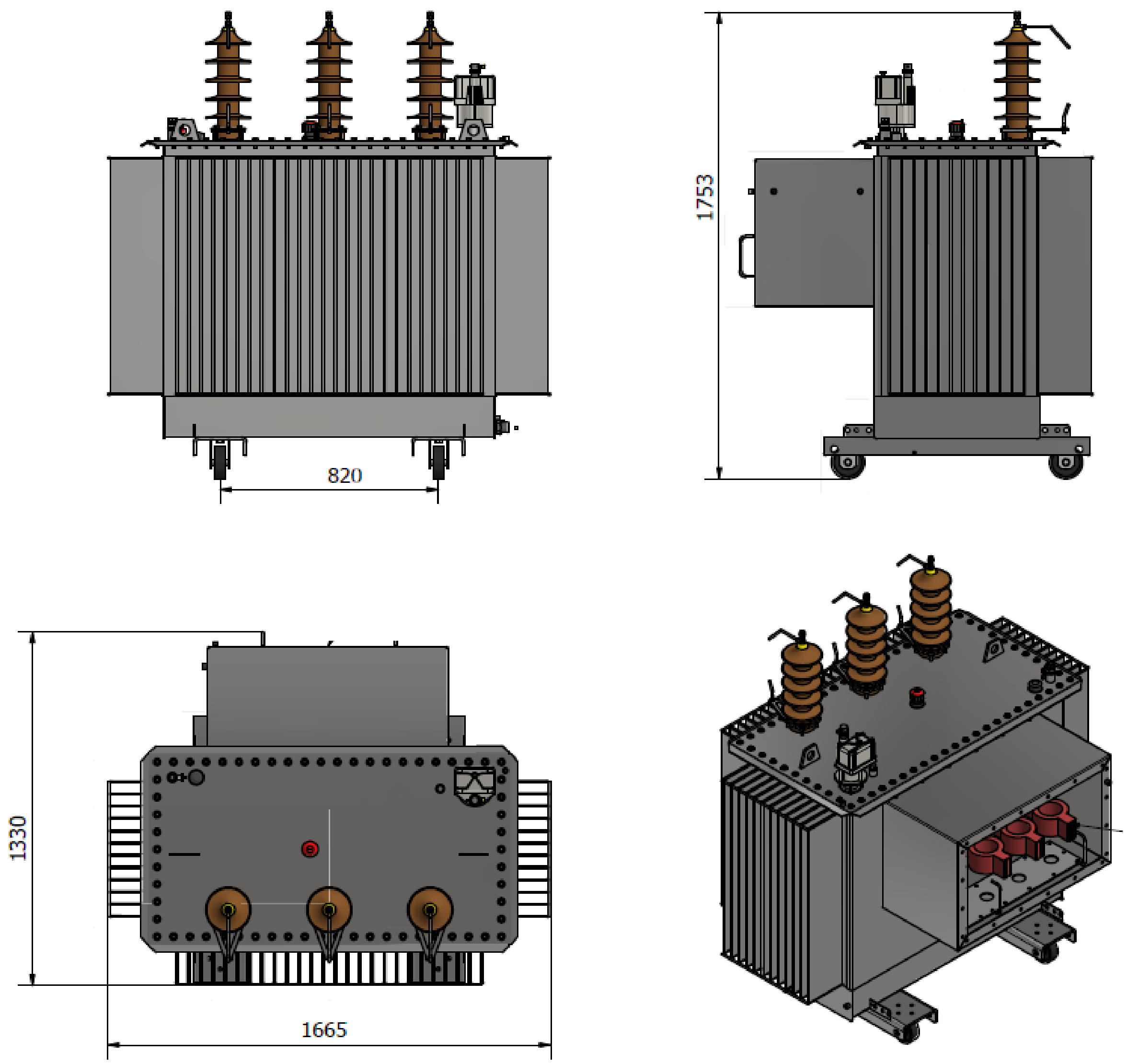

Figure 3.22. The boiler, frame and cover (3D view)

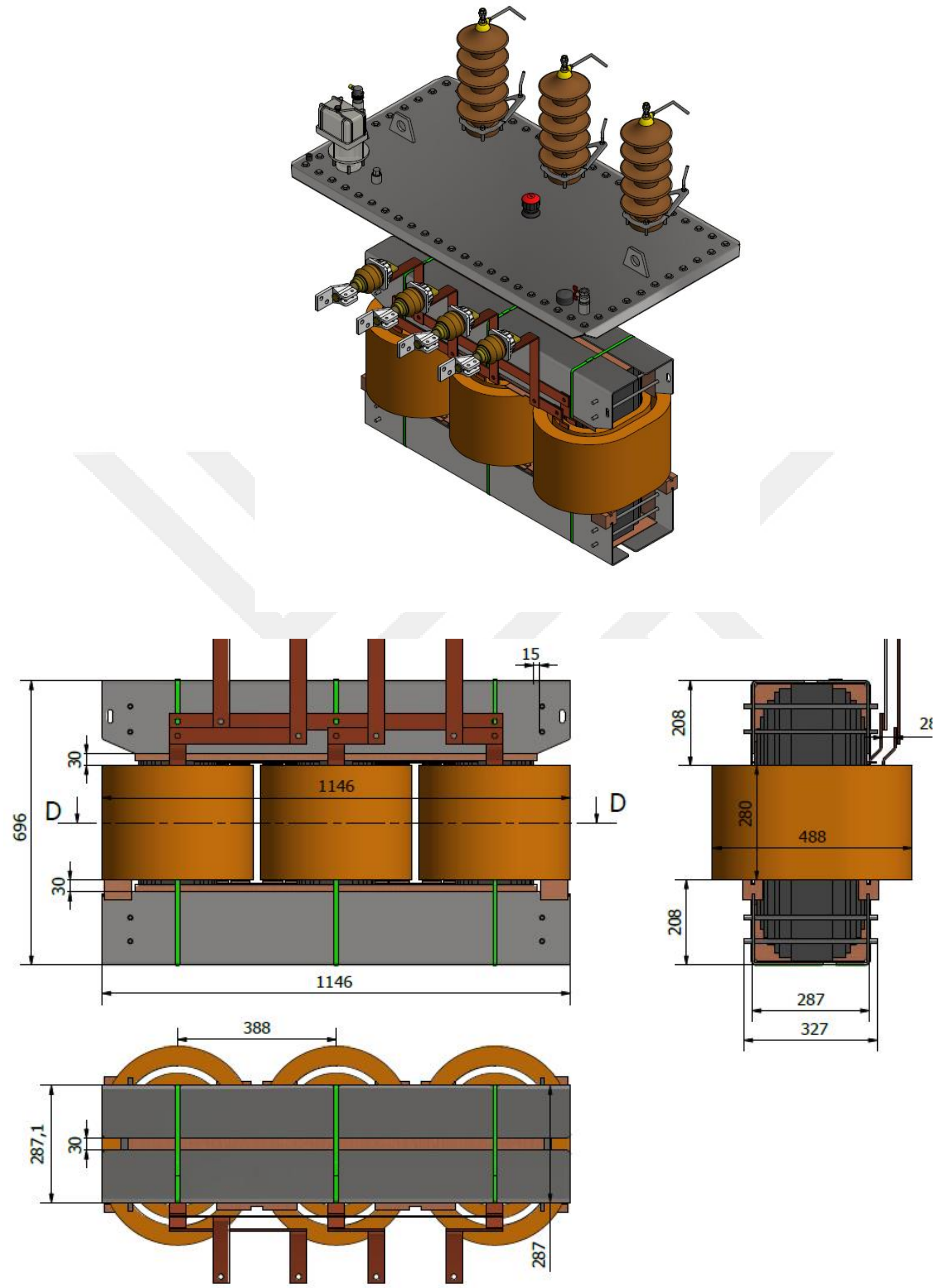

Figure 3.23. The active part of the transformer (3D view)

3.3. Thermal Design

The ONAN cooling method was used for the cooling type of the transformer. To dissipate the heat that may occur from the sum of load, no-load, and other losses, wave walls and boiler surfaces made of 1.2 mm thick DKP sheet metal are used.

Because the core is inner than the windings, the temperature rise occurs later and more than in the coils. The low-voltage gradient was 15 K, and the high-voltage gradient was 13 K. The temperature increases of the oil and windings reached a maximum of 55 °C and 60 °C, respectively. According to the design results, the peak oil temperature is 33 °C at 1.522 Tesla. The temperature curves of the transformer are shown in Figure 3.24.

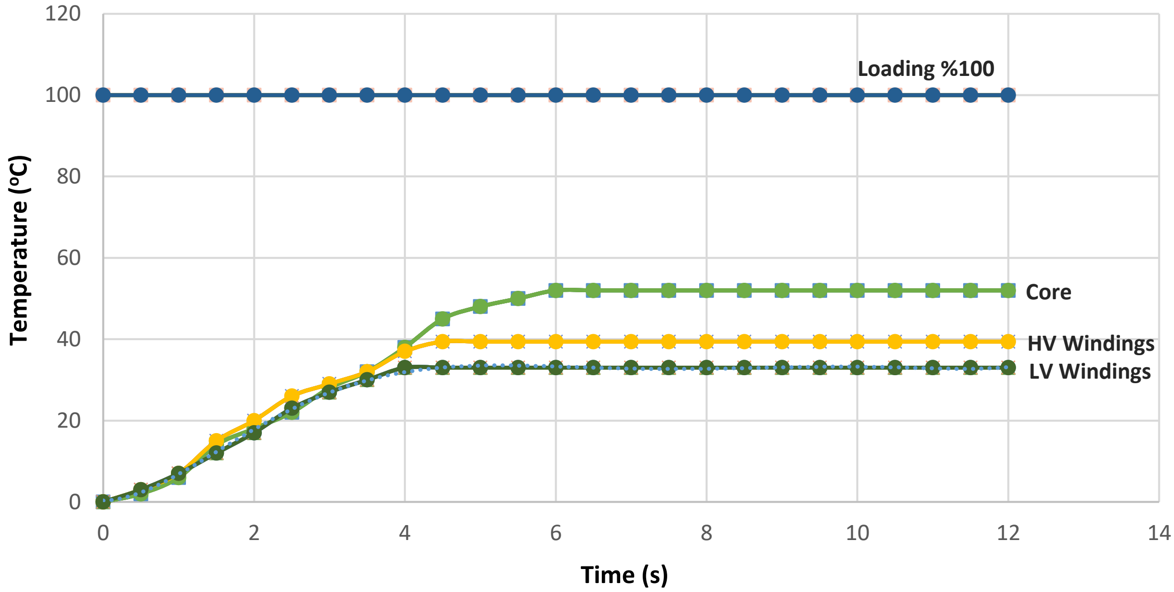

Figure 3.24. The temperature curves

3.4. Manufacturing Process

The manufacturing process of a CSP transformer consists of four steps. First, the transformer coils are wound considering the bobbin project. Second, the core of the transformer is cut into core-cutting machines and arranged according to the assembly project. In the third step, other mechanical parts are manufactured. In the fourth step, the active part is assembled, and a prototype is obtained.

3.4.1. Winding Manufacturing

The low-voltage winding is one of the first stages of winding manufacturing, and the winding is applied with foil or flat conductive material in a cross-section determined according to the transformer current on the mold prepared before production. To provide insulation between the windings, dried kraft paper coated with resin called DDP was used. Owing to the channel rods placed between the layers, an oil flow is provided between the windings and efficient cooling is provided. Interlayer cooling ducts (axial and radial) are provided to minimize the temperature difference between the windings and oil; hence, the hot spot temperature is kept to a minimum. This also ensures that the rate of insulation deterioration is minimized and a high life expectancy is achieved. Transpositions are performed in multiple conductor windings to ensure uniform current distributions, minimize circulating currents, decrease eddy current loss, and improve the lamination factor. Figure 3.24 shows the low-voltage winding production stage.

After low-voltage winding manufacturing is completed, high-voltage winding manufacturing is performed, as shown in Figure 3.25. This process is conducted in the high-voltage winding department in accordance with the materials specified in the enameled prescription and the number of windings designed in the project. The coil is wound in automatic winding machines, with the conductor cross-section determined according to the current value in the high-voltage section. After this process, the high-voltage coil is completed. The coils are then examined for visual and dimensional conformities. They are kept in a suitable area for assembly in another section.

Specialized disc windings and interleaved disc windings have a very high series capacitance, giving a very good impulse voltage performance. To improve the short-circuit withstandability under fault conditions, the coils are pressed, clamped, and dried in an oven before impregnation in oil. Cooling ducts formed with rigid, high-density spacers, and horizontal and vertical ducts are provided to save hot spots.

Figure 3.24. Low-voltage winding production

Figure 3.25. High-voltage winding production

3.4.2. Magnetic Core Manufacturing

The most important material in a transformer is its core. The core is formed by combining CRGO silicone sheets with high magnetic permeability in a certain order. The type of magnetic steel is chosen according to the desired loss level. The sheet metal type used for the idle loss value determined in the project is selected as M4.

The laminations are cut geometrically to ensure an optimum magnetic flux flow and a minimum air gap between the joints of two consecutive sheets. The supporting structures and clamping devices of the core contribute to the compactness of the design and ensure low sound levels. The core is designed with a safe flux density to minimize core loss and magnetizing current. But-lap, miter, or step-lap-miter construction is chosen based on the application and core-loss requirements. Laminations are burr free fully annealed with low loss and very thin between 0.23 mm and 0.30 mm, varying no more than + 0.05 mm in length for the lowest sound level and excitation currents. Each lamination is covered with a high-resistance, inorganic coating to reduce the eddy currents.

Following the core cross-section and step numbers specified in the project, pieces of the core are cut into automatic core-cutting machines and stacked by the machine. Care is taken to ensure that there are no burrs on the core parts and that the sheet is not damaged in a way that would disrupt the existing flux structure. Figure 3.26 illustrates an image of the core cutting and storage.

Figure 3.26. Core Cutting Stage

The cut and stored core parts are stacked on top of each other, considering the dimensions of the project, to place the completed coils, and their upper and lower parts are supported with the help of iron material. Care is taken to ensure that there are no gaps between the core parts and that the measurement tolerances are not exceeded. The core alignment stages are demonstrated in Figure 3.27. The aligned core is lifted up with the help of a crane and prepared for the assembly of the coils, as shown in Figure 3.28.

Figure 3.27. Core Alignment Stage

Figure 3.28. Core Assembly Stage

3.4.3. Manufacturing of Other Mechanical Parts

While the electrical production stages are completed, the production of the necessary materials for the mechanical section is also carried out. As seen in Figure 3.29, the pan, which is the bottom base of the boiler, and the carrier parts that ensure the integrity of the coil-core structure, which is considered the active part, are cut in the laser cutting machine according to the mechanical project dimensions. Figure 3.30 shows that the parts to be used for fixing between the active part and boiler are being cut. Mechanical parts approved by the quality control unit are taken to the next section for welding.

Figure 3.29. Tank base and carrier cutting stage

Figure 3.30. Twisting of boiler fixing apparatus

Figure 3.31 demonstrates the production phase of the frame. The frame is used between the boiler and the cover, where the sealing gasket is located. It is cut using a laser machine and prepared for welding.

Figure 3.31. Frame manufacturing stage

The boiler is created by welding parts prepared for the mechanical section using a laser machine in the welding department. The completed boiler, shown in Figure 3.33, is delivered to the paint shop department for the painting process after leakage testing, and visual checks are carried out by the quality control unit.

Figure 3.32. The image of boiler

3.4.4. Assembly of the Active Part

The coils formed by the low and high-voltage windings are cut and arranged. It is placed on each leg of the standing core and compressed with upper clamps, and the active part is completed.

At this stage, the accuracy of the winding number is confirmed by performing ratio tests. As shown in Figure 3.33, fuses intended for use in the CSP transformer are placed on the wedges on the active part. The coil connection of the busbars required for a low-voltage bushing connection is carried out.

Figure 3.33. Assembly of the active part

The boiler and cover, painted using the electrolytic powder coating method, are placed in the final assembly area and assembled with the active part. Low-high-voltage bushings and protection elements are assembled and made ready for oil filling, as shown in Figure 3.34-36.

Figure 3.34. CSP transformer prototype (Front view)

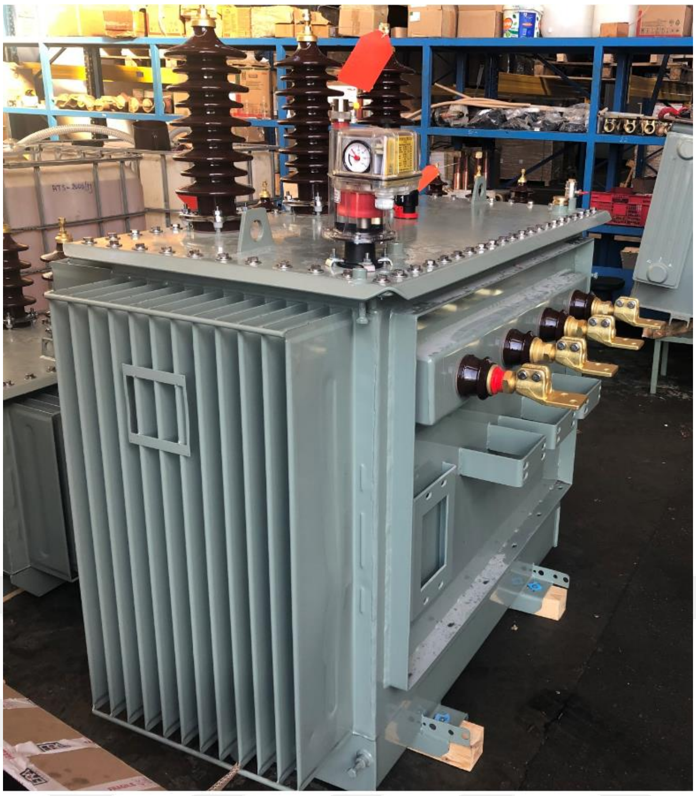

Figure 3.35. CSP transformer prototype (Side view)

Figure 3.36. CSP transformer prototype (Rear view)

After the oil filling is done, the prototype is kept in the waiting area for oil absorption and rest, and then it is taken to the test section and test preparations are made.

The standards that the developed transformer complies with are as follows:

- IEC 66076-1 Power transformers - Part 1: General
- IEC60076-2 Power transformers - Part 2: Temperature rise
- IEC 60076-3 Power transformers - Part 3: Insulation level - Dielectric tests and External clearances in air
- IEC 60076-3 Power transformers - Part 4: Guide to the lightning impulse and switching impulse testing-Power transformers and reactors
- IEC60076-5 Power transformers - Part 5: Ability withstand short circuit
- IEC60076-8 Power transformers -Part 8: Application guide
- IEC60076-10 Power transformers - Part 10: Determination of sound levels
- IEC60076-13 Power transformers - Part 13: Self-protected liquid-filled transformers
- IEC60214-1 Tap-changers - Part 1: Performance requirements and test methods
- IEC60296 Fluids for Electrotechnical applications-Unused mineral insulating oils for transformers and switchgear
- IEC 60354 Loading guide for ol-immersed power transformers
- IEC 60567 Guide for the sampling of gases and of oil from oil filled electrical equipment and for the analysis of free and dissolved gases
- Current transformers
- IEC 60137 Insulated bushing for alternating voltages above 1000 volts
- IEC 60156 Insulating liquids -Determination of the breakdown voltage at power frequency

4. RESULTS AND DISCUSSIONS

The performance of the CSP transformer is evaluated through routine, type, and special tests. The routine tests include measurement of winding dc resistance, measurement of short-circuit losses and short-circuit impedance, measurement of no-load ratio and control of polarity, applied voltage test, and induced voltage test.

Table 4.1 shows the winding resistance measurement results for the CSP transformer. The changes in low and high voltage winding resistances over time is presented in Figure 4.1. By measuring the winding resistances of the transformer, the accuracy of many important parameters such as winding and assembly errors and conductor defects can be confirmed. This is why it is very important that it constitutes the first of the testing stages.

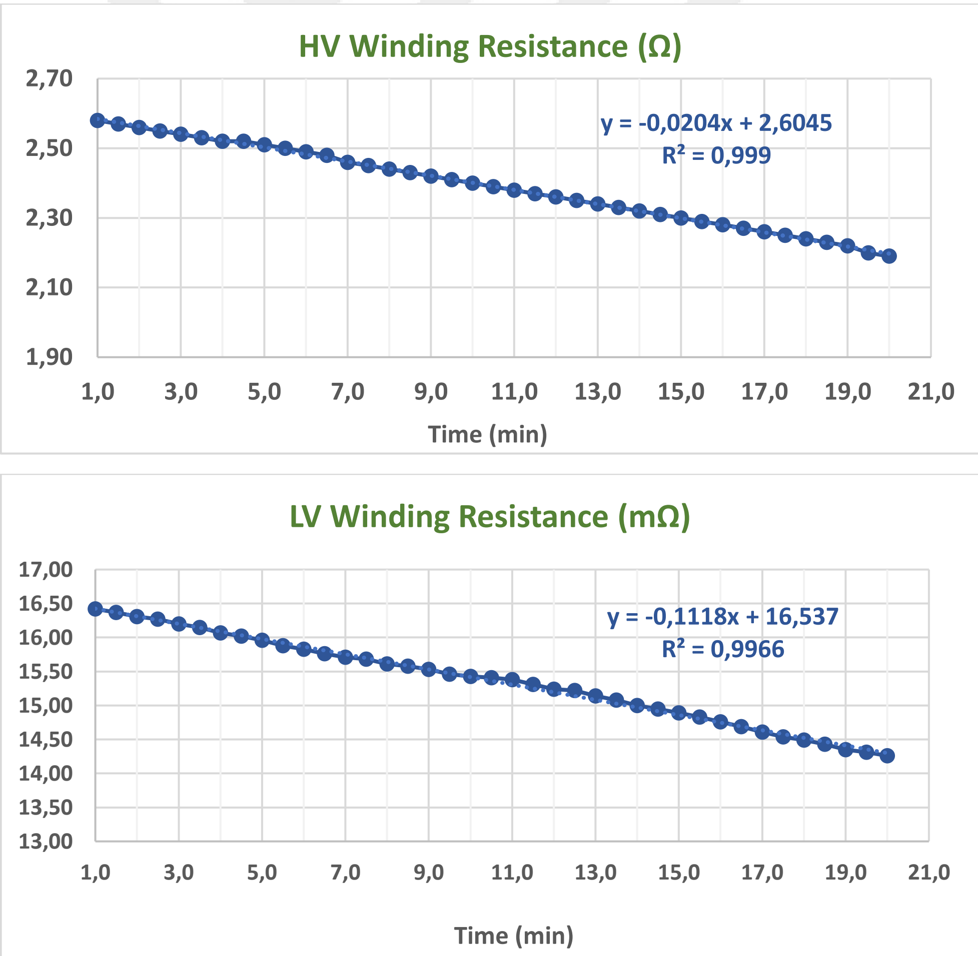

Figure 4.1. The graphs of low and high voltage winding resistances over time

Table 4.1. Measurement results of time-dependent winding resistances (Routine test 1)

	LV Winding resistances		HV Winding Resistances	
Measurement	**Time (min)**	**Resistance (mΩ)**	**Time (min)**	**Resistance (Ω)**
1	1,0	16,42	1,0	2,58
2	1,5	16,37	1,5	2,57
3	2,0	16,31	2,0	2,56
4	2,5	16,27	2,5	2,55
5	3,0	16,20	3,0	2,54
6	3,5	16,15	3,5	2,53
7	4,0	16,07	4,0	2,52
8	4,5	16,02	4,5	2,52
9	5,0	15,96	5,0	2,51
10	5,5	15,88	5,5	2,50
11	6,0	15,83	6,0	2,49
12	6,5	15,76	6,5	2,48
13	7,0	15,71	7,0	2,46
14	7,5	15,68	7,5	2,45
15	8,0	15,61	8,0	2,44
16	8,5	15,58	8,5	2,43
17	9,0	15,53	9,0	2,42
18	9,5	15,46	9,5	2,41
19	10,0	15,43	10,0	2,40
20	10,5	15,41	10,5	2,39
21	11,0	15,38	11,0	2,38
22	11,5	15,31	11,5	2,37
23	12,0	15,24	12,0	2,36
24	12,5	15,22	12,5	2,35
25	13,0	15,14	13,0	2,34
26	13,5	15,08	13,5	2,33
27	14,0	15,00	14,0	2,32
28	14,5	14,95	14,5	2,31
29	15,0	14,89	15,0	2,30
30	15,5	14,83	15,5	2,29
31	16,0	14,76	16,0	2,28
32	16,5	14,69	16,5	2,27
33	17,0	14,61	17,0	2,26
34	17,5	14,54	17,5	2,25
35	18,0	14,49	18,0	2,24
36	18,5	14,43	18,5	2,23
37	19,0	14,35	19,0	2,22
38	19,5	14,31	19,5	2,20
39	20,0	14,26	20,0	2,19

Table 4.2 summarizes the average winding resistance values for the CSP transformer at t = 16.4 ^{0}C. The losses that occurred according to these values are listed in Table 4.3.

Table 4.2. Average winding resistance values (Routine test 1)

High Voltage Coil Resistance		
TS EN 60076-1 / 11.2		t = 16,4 ºC
RUV (Ω)	RVW (Ω)	RWU (Ω)
13,837	13,844	13,834
Low Voltage Coil Resistance (mΩ)		
TS EN 60076-1 / 11.2		
ruv	rvw	rwu
2,172	2,175	2,171

Table 4.3. Losses (Routine test 2)

Losses	
No Load Losses (W)	970
Short Circuit Losses at 75 ºC (W)	4199
Total Losses (W)	5210

The short-circuit impedance is the ratio of the voltage passing through the primary windings to the nominal voltage generated by short-circuiting the secondary windings. The transformer needs to operate efficiently such that the short-circuit impedance is within the percentage tolerances determined by the national standards (IEC).

Table 4.4 provides the measurement results of short-circuit voltage and load losses. When the short-circuit impedance is obtained, the voltage value with the nominal current value is also the load loss value. Losses in the load can be considered as losses in the winding resistances, core, boiler (mechanical parts), and connection points. As can be seen in the measurement results, the loss at the load predicted to be 4250 W has been measured as 4199 W. This is within the percentage tolerances determined by national standards (IEC).

Table 4.4. Measurement of Short-Circuit Voltage and Load Losses Values (Routine test 3)

Short-Circuit Voltage and Load Losses Values TS EN 60076-1:2012 / 11.4								
TAP	Current Tr. Multip.	Voltage Tr. Multip.	Voltage (V)	Current (A)	Wattmeter (W)	P (kW)	% Uk 75°C	P 75°C (W)
3	1	20	1661,2	8,742	3585,5	3,5855	5,05	4199

Guarantee % short circiut voltage (75 °):	5	Guarantee % load losses (75°):	4250 W

The measurement of no-load losses and no-load current is performed to analyze the iron losses that occur when the transformer is not active. The most important iron losses are magnetization, fuko, and hysteresis. With no-load loss test, comments can be made regarding the core sheet quality and alignment.

When the primary windings are idle, the rated voltage is applied to the secondary windings, and after a certain period of time, the voltage drawn from each phase of the secondary windings is measured and summed to obtain idle losses. The average of the current values drawn from each phase is the idle current value. As stated in the measurement results given in Table 4.5, the guaranteed idle loss value was 1000 W, whereas the idle loss was measured as 970.4 W. This is within the percentage tolerances determined by national standards (IEC).

Table 4.5. Measurement of No-Load Losses and Current Values (Routine test 4)

No-load Losses and Current Values TS EN 60076-1:2012 / 11.5					
Current Tr. Multip:	1	U1 = 432,8 V	I1 = 2,48 A	Iort = 2,42 A	% Io = 0,36
Voltage Tr. Multip:	20	U2 = 432,8 V	I2 = 2,17 A	**Meas. Value**	No-load losses in guarantee
		U3 = 432,8 V	I3 = 2,61 A	Pb = 970,4 W	Pb = 1000 W

Table 4.6 lists the test results for the no-load ratio and polarity control. The turn ratio confirms the accuracy of the number of windings of the transformer. The voltage conversion ratio designed for each tap shows that the intended values have been successfully achieved using this test. The ratios in the measurement results are within the tolerances of national standards. Polarity is a test in which the connection group and direction of winding connections are determined.

Table 4.6. No-load ratio and control of polarity test (Routine test 5)

Tap	**No Load Ratio**	**No-Load Ratio Values TS EN 60076-1:2012 / 11.3**			**No-Load Ratio Fault %**		
		UV/uv	**VW/vw**	**WU/wu**	**UV/uv**	**VW/vw**	**WU/wu**
1	125,400	125,40	125,40	125,41	0,000	0,000	0,008

2	128,700	128,69	128,70	128,70	-0,008	0,000	0,000
3	132,000	132,02	132,01	132,01	0,015	0,008	0,008
4	135,300	135,30	135,30	135,30	0,000	0,000	0,000
5	138,600	138,60	138,60	138,60	0,000	0,000	0,000

With the applied voltage test, the insulation between the LV-HV windings, windings and boiler, core and windings are tested. Whether the jumping distances are sufficient is tested by applying voltage to the HV winding. The most important criterion is that no arc occurs between these sections. The voltage level to be applied is determined on the basis of the kV levels determined by the IEC. For the 33 kV rated transformer, 70 kV is applied to the HV winding for 1 min. If there is no jump during the test, the applied voltage remains constant for 1 min and the production is proven to be successful.

The insulation between the windings is tested by the induced voltage test. A voltage twice the nominal voltage is applied to the secondary winding. The frequency is doubled to prevent the core from saturating during the test. The duration of the test is obtained by the ratio of the rated frequency to the tested frequency. Since the converter in the laboratory is 200 Hz, two times the nominal voltage is applied to the CSP transformer for 30 seconds. Table 4.7 presents the results of applied and induced voltage tests.

Table 4.7. Applied voltage test, and induced voltage test (Routine test 6)

<table>
<tr><td rowspan="2">Applied Voltage Experiment
IEC 60076-3:2013 / 10</td><td>HV Coil (kV)</td><td>LV Coil (kV)</td><td>f= 50 Hz</td><td rowspan="2">Induced Voltage Experiment
IEC 60076-3:2013 / 11</td><td>U=866,1 V</td><td>F = 200 Hz</td><td>t= 30 sec</td></tr>
<tr><td>70</td><td>3</td><td>t= 60 sec</td><td colspan="3">OK</td></tr>
</table>

The type tests include temperature rise and lightning impact tests presented in Table 8 and 9.

Table 4.8. Temperature rise test (Type Test 1)

		HV	LV
Oil temperature at upper point of transformer after the rated current (°C)	Tynom	62,6	62,6
Maximum oil temperature at upper point of transformer (°C)	Tymax	63,4	
Ambient temperature after the rated current (°C)	Tortnom	16,6	16,6
Ambient temperature while oil rise max.temp. (°C)	Tortmax	15,5	

Upper radiator temperature while oil rise max.temp. (°C)	Trüm (upper)	54,6	54,6
Lower radiator temperature while oil rise max.temp (°C)	Tram (lower)	45,2	45,2
Temperature changing at cooling system while oil rise max.temp. (Trüm-Tram)/2 (°C)	ΔTrm	4,7	
Upper radiator temperature after the rated current (°C)	Trün	54,6	54,6
Lower radiator temperature after the rated current (°C)	Tran	45,1	45,1
Temperature changing at cooling system after the rated current (Trün-Tran)/2 (°C)		4,8	
Tymax-Tynom (°C)	ΔΘ		
DC Resistance (Ω)	R (measuring)		
Resistance at end of the test (calculated with graphs and slope) (Ω)	Ro (extrapolation)		
Temperature of winding at end of the test (calculated from resistance changing)	Tr (calculation)		
Winding temperature while max.oil temp. (°C)	Trd Tr-ΔΘ		

Table 4.9. Lightning impulse test (Type Test 2)

Lightning Impulse Test				
TS EN 60076-3:2014 Madde 13, TS EN 60076-3/A1:2018, IEC 60076-3:2013 / 13, IEEE Std. C57.12.90:2015 / 10.3				
NO	**Up (kV)**	**T1 (µs)**	**T2 (µs)**	**Description**
1	-103,74	1,21	40,46	reference voltage between 50% and 70%
2	-173,00	1,26	41,66	Phase U, first impulse
3	-174,82	1,34	41,89	Phase U, second impulse
4	-172,78	1,33	46,06	Phase U, third impulse
5	-173,72	1,34	45,81	Phase V, first impulse
6	-172,41	1,32	45,22	Phase V, second impulse
7	-171,95	1,30	46,11	Phase V, third impulse
8	-173,73	1,33	44,39	Phase W, first impulse
9	-168,84	0,90	50,38	Phase W, second impulse
10	-168,57	0,90	50,48	Phase W, third impulse

The special tests include capacity and loss angle tan(φ) measurement, insulation resistance measurement, measurement of noise level, no-load current and harmonic components measurement, and oil dielectric strength measurement. The aforementioned tests have been performed for the produced CSP transformer and the test results are presented in Table 4.10, Table 4.11, Table 4.12, Tablo 4.13 and Table 4.14.

Table 4.10. Capacity and loss angle tan(φ) measurement (Special Test 1)

Power:	500 kVA	Phase Num.:		3	Freq: 50 Hz	
Primary Voltage:	33 kV	Secondary Voltage:		0,433 kV	t = 19,4 ºC	
Capacity and Tan δ Measurement TS EN 60076-1 IEC 60076-1 IEEE Std C57.12.90 /.10.10						
Measured	Test Voltage (kV)	Measured				
		mA	Watt	tanδ	Capacity (Cp) (F)	Power Factor (% PF)
CH (HV-T)	9,996	12,28	0,271	0,291	3,974	0,291
CHL (HV-LV)	9,999	29,784	0,718	0,264	9,495	0,264
CH+CHL (HV+HV-LV)	9,987	42,263	0,994	0,266	13,976	0,266
CL (LV-T)	2,010	6,523	0,037	0,261	10,417	0,261

Table 4.11. Insulation resistance measurement (Special Test 2)

Insulation resistance (Giga Ohm) IEEE Std. C57.12.90:2010 / 10.11						
t = 18,9 °C			Correction factor for reference temperature of 20°C		K= 0,86	
Time	5000 V H.V.-T	Account	5000 V H.V.-L.V.	Account	2500 V L.V.-T	Account
0 s	9,46	8,14	11,96	10,29	4,54	3,90
15 s	16,76	14,41	18,46	15,88	10,74	9,24
30 s	22,46	19,32	24,56	21,12	18,54	15,94
45 s	28,66	24,65	30,36	26,11	26,14	22,48
60 s	34,96	30,07	35,76	30,75	34,94	30,05

Table 4.12. Measurement of noise level

Transformer Details		**Measuring Device Details**	
Serial Number:	104344	Mark:	CEM
Power:	500 kVA	Type:	Sound Level Meter
Taps:	31,35 - 32,175 - 33 33,825 - 34,65	Serial Number:	130726861
Nominal Primary Voltage:	33 kV		
Nominal Level:	3		
Test Voltage:	0,433 kV		
Vector Group:	DYN-11		

Type of Cooling:	ONAN	
Frequency:	50 Hz	

Measurement Results

Plan Location	dB 1	dB 2	dB 3	Plan Location	dB 1	dB 2	dB 3	Plan Location	dB 1	dB 2	dB 3	Plan Location	dB 1	dB 2	dB 3
1	54,8	54,7	54,6	13				25				37			
2	54,7	54,5	54,5	14				26				38			
3	54,4	54,1	54,1	15				27				39			
4	54,5	54,4	54,3	16				28				40			
5	54,6	54,3	54,1	17				29				41			
6	54,4	-0,1	-0,1	18				30				42			
7	54,7	-0,1	-0,1	19				31				43			
8	54,5	-0,1	-0,1	20				32				44			
9				21				33				45			
10				22				34				46			
11				23				35				47			
12				24				36				48			

1=Device Sound, 2=Location Sound before test, 3=Location sound after test	**Arithmetic Average**	54,68	34,06	34,01

Length in meters of the transformer tank (h):	1,12
Basic diffusion surface (Im):	0,3
Absorption coefficient (a):	0,2
Surface area (Sv):	12690
Sound absorption area (A):	2538
Height above the ground in microphone (m):	0,56

Correction Related to the Environment, K	**0,002873811**		LpA (dB)	**54,63**

Active Surface Arena				
a-) For measurements at a distance of 0.3 m from the fundamental radiation surface	0,42	m^2	10 log 10 S/S0	**-3,77**
a-) For measurements at a distance of 2 m from the fundamental radiation surface	………..	m^2		
a-) For measurements at a distance of 1 m from the fundamental radiation surface	………..	m^2	LwA(dB)	**51**

This transformer is suitable for standards (TS EN 60076-10)

Table 4.13. No-load current and harmonic components measurement

Power:	500 kVA	**Phase Number:**	3	**Frequency:**	50 Hz

Tap	Primer Voltage (HV)	Seconder Voltage (LV)	Primer Current (A)	Seconder Current (A)
1	31350		9,208	
2	32175		8,972	
3	33000	433	8,748	666,7
4	33825		8,535	
5	34650		8,331	

Measurement of the harmonics of the no-load current

Current Tr. Multip:		10		**U1 =**	432,7 V		**I1 =**	2,482 A	
Volt. Tr. Multip:		20		**U2 =**	432,7 V		**I2 =**	2,168 A	
Wttm. Multip:		200		**U3 =**	432,6 V		**I3 =**	2,617 A	
	2	**3**	**4**	**5**	**6**	**7**	**8**	**9**	**10**
I1	0,822 A	0,002 A	0,434 A	0,003 A	0,327 A	0,003 A	0,216 A	0,003 A	0,187 A
I2	0,730 A	3E-16 A	0,364 A	0,001 A	0,286 A	0,001 A	0,185 A	0,001 A	0,163 A
I3	0,874 A	0,002 A	0,484 A	0,002 A	0,308 A	0,002 A	0,203 A	0,002 A	0,181 A
Total Harmonic Content				**I1**	0,412 A	**Guaranteed Value**		**0,43**	
				I2	0,413 A				
				I3	0,412 A				
This transformer is suitable for standards (TS EN 60076-1,IEC 60076-1,IEEE Std. C57.12.90)									

Table 4.14. Oil dielectric strength measurement

OIL							
					Type	SHELL DIALA	
Insulating liquids **(kV/2,5 mm)** TS 3989 EN 60156:1998							
73,6	73,2	70,7	67,6	68,8	70,4	Uort =	71

To determine the electrical strength of the oil, the dielectric strength of the oil was measured and evaluated in kilovolts. The voltages applied to the oil penetration device and the oil sample must meet the threshold values specified in the IEC.

In addition to these tests, connections between the hardware and equipment used to protect the transformer are tested to confirm their functionality. The micron thickness of the paint is confirmed with at least three points taken from the transformer boiler. It is also important that the coating thicknesses are appropriate, and that the paint surface has a monolithic structure.

5. CONCLUSIONS

The distribution transformer emerges as a critical component within the power distribution system, ensuring the delivery of reliable and demanded levels of voltage to the final consumers. The critical nature of distribution transformers becomes particularly apparent when viewed through the lens of the end-user experience. Residential, commercial, and industrial consumers depend on consistent and reliable power supplies for their activities. Any disruption or inefficiency in the operation of the distribution transformers may result in potential interruptions or fluctuations in the power supplied to these diverse consumer segments.

Protection approaches for distribution transformers vary based on their size and type. Typically, mechanical relays such as the Buchholz relay and sudden pressure relay protection are applied to transformers with a capacity of 0.5 MVA and above. These mechanical relays detect faults that are undetectable by the main relay. Smaller distribution transformers primarily use high-voltage fuses as the primary protective device. For transformers of up to 1000 kVA (used in 11 kV and 33 kV distribution), fuses and medium-voltage circuit breakers are frequently employed. Larger and more crucial distribution transformers benefit from overcurrent protection combined with restricted earth fault protection. Transformers rated above 10 MVA usually incorporate differential protection, where the current differential relays act as the primary safeguard. As a backup protection measure, distance protection, overcurrent protection (phase current, zero-sequence current), or a combination of both are commonly applied. Additionally, thermal overload protection is often utilized to prolong the lifespan of the transformer rather than solely for fault detection. In traditional distribution transformers, supplementary equipment, such as disconnectors, breakers, and surge arresters, are externally installed to enhance system protection.

The concept of CSP technology is well recognized for its application in high-performance distribution transformers. This technology facilitates seamless operation and minimizes the maintenance and operational issues commonly associated with distribution transformers. A CSP transformer is designed to autonomously protect itself from faults on the low-voltage side (typically the secondary side), lightning-related issues caused by surge arresters, and overloads on the high-voltage side. Moreover, it provides a clear warning of overload conditions through a signal light. CSP methods extend their protective capabilities to the connected distribution system, thereby enhancing the overall resilience of the system to which the transformer is linked.

In this thesis, a 500 kVA, 33/0.4 kV CSP distribution transformer has been designed and implemented. The design stages are detailed in terms of electrical, thermal, and mechanical properties. Following the design stages, the manufacturing processes are presented. The produced prototype has been tested with routine, type, and special tests. The details of the related tests and test results have been presented.

As a combination of the existing CSP designs, protection is provided by the interrupter on the primary side and by the circuit breaker in the cable box to be located on the secondary side. This eliminates the need for an oil type circuit breaker. The protection system is located internally on the transformer. The thermal protection system protects against long-term overload. In the case of a fault, the transformer isolates itself from the connected distribution network, minimizing the impact on only the affected loads. The inclusion of a signal lamp on the transformer informs the distribution system operator about the requirement to switch to a higher power setting. Furthermore, surge arresters, strategically positioned on the transformer tank, enhance protection against lightning strikes.

REFERENCES

[1] S. V. Kulkarni, and S. A. Khaparde, Transformer Engineering: Design, Technology, and Diagnostics (2nd ed.), 2017, doi: 10.1201/b13011.

[2] V. Lebedev, "Transformer Basics", 2007 Electrical Insulation Conference and Electrical Manufacturing Expo, 2007, doi: 10.1109/EEIC.2007.4562642.

[3] J. Feng, W. Q. Chu, Z. Zhang and Z. Q. Zhu, "Power Electronic Transformer-Based Railway Traction Systems: Challenges and Opportunities," IEEE Journal of Emerging and Selected

Topics in Power Electronics, vol. 5, no. 3, pp. 1237-1253, Sept. 2017, doi: 10.1109/JESTPE.2017.2685464.

[4] S. Enache, A. Campeanu, M. A. Enache, I. Vlad and M. Popescu, "Optimizing Design of Transformers Used in Railway Traction," 2020 International Conference and Exposition on Electrical And Power Engineering (EPE), Iasi, Romania, 2020, pp. 253-258, doi: 10.1109/EPE50722.2020.9305531.

[5] N. Chowdhury and M. Mann, "Estimating the impact of a residential microgrid on distribution transformer," 2019 2nd International Conference on Power Energy, Environment and Intelligent Control (PEEIC), Greater Noida, India, 2019, pp. 513-517, doi: 10.1109/PEEIC47157.2019.8976472.

[6] G. C. Jaiswal, P. A. Venikar, M. S. Ballal, H. M. Suryawanshi and D. R. Tutakne, "Smart transformers for industrial applications," 2017 IEEE Transportation Electrification Conference (ITEC-India), Pune, India, 2017, pp. 1-4, doi: 10.1109/ITEC-India.2017.8333713.

[7] F. Poza, P. Marino, S. Otero and V. Pastoriza, "Instrumentation system for industrial [transformers," 2008 10th International Conference on Control, Automation, Robotics and Vision, Hanoi, Vietnam, 2008, pp. 1929-1933, doi: 10.1109/ICARCV.2008.4795824.

[8] E. Rotholz, "Transmission-Line Transformers," in IEEE Transactions on Microwave Theory and Techniques, vol. 29, no. 4, pp. 327-331, Apr. 1981, doi: 10.1109/TMTT.1981.1130352.

[9] G. Crotti, G. D’Avanzo, P. S. Letizia and M. Luiso, "The Use of Voltage Transformers for the Measurement of Power System Subharmonics in Compliance With International Standards," IEEE Transactions on Instrumentation and Measurement, vol. 71, pp. 1-12, 2022, Art no. 9005912, doi: 10.1109/TIM.2022.3204318.

[10] T.K. Ganguli, "Transformers : Design, Manufacturing, and Materials" by Bharat Heavy Electrical Limited, McGraw-Hill, 2004.

[11] https://www.technicalbookspdf.com/losses-in-transformers-hysteresis-loss-eddy-current-loss-efficiency/

[12] J. de Oliveira Quevedo et al., "Analysis and Design of an Electronic On-Load Tap Changer Distribution Transformer for Automatic Voltage Regulation," IEEE Transactions on Industrial Electronics, vol. 64, no. 1, pp. 883-894, Jan. 2017, doi: 10.1109/TIE.2016.2592463.

[13] W. Hejian, L. Hongtao, G. Tao, J. Jun, Z. Hailong and J. Song, "Research and Application of 10kV Built-in High Voltage Protection Distribution Transformer," 2018 China International Conference on Electricity Distribution (CICED), Tianjin, China, 2018, pp. 280-284, doi: 10.1109/CICED.2018.8592468.

[14] O. Özgönenel, G. Önbilgin, Ç. Kocaman, “Transformer Protection Using the Wavelet Transform” Turkish Journal of Electrical Engineering, vol.13, no.1, pp. 119-135, 2005.

[15] V. B. Martin and J. R. Marek, "An Economical Coordinated Scheme for Complete Transformer Protection," IEEE Transactions on Power Delivery, vol. 2, no. 4, pp. 1244-1248, Oct. 1987, doi: 10.1109/TPWRD.1987.4308247.

[16] S. Jhunjhunwala, K. Pandey and R. Kumar, "A Microcontroller Based Embedded System to Provide Complete Self Protection (CSP) to any Distribution Transformer," 2018 International Conference on Power Energy, Environment and Intelligent Control (PEEIC), Greater Noida, India, 2018, pp. 307-310, doi: 10.1109/PEEIC.2018.8665655.

[17] D. Wang et al., "A New Testing Method for the Dielectric Response of Oil-Immersed Transformer," IEEE Transactions on Industrial Electronics, vol. 67, no. 12, pp. 10833-10843, Dec. 2020, doi: 10.1109/TIE.2019.2959500.

[18] A. A. Taheri, A. Abdali and A. Rabiee, "A Novel Model for Thermal Behavior Prediction of Oil-Immersed Distribution Transformers With Consideration of Solar Radiation," IEEE Transactions on Power Delivery, vol. 34, no. 4, pp. 1634-1646, Aug. 2019, doi: 10.1109/TPWRD.2019.2916664.

[19] S. Okabe, G. Ueta and T. Tsuboi, "Investigation of aging degradation status of insulating elements in oil-immersed transformer and its diagnostic method based on field measurement data," IEEE Transactions on Dielectrics and Electrical Insulation, vol. 20, no. 1, pp. 346-355, February 2013, doi: 10.1109/TDEI.2013.6451376.

[20] L. Jin, D. Kim and A. Abu-Siada, "State-of-the-art review on asset management methodologies for oil-immersed power transformers," Electric Power Systems Research, vol. 218, 109194, 2023, doi: 10.1016/j.epsr.2023.109194.

[21] C. Lin, C. Wu and P. Huang, "Grey clustering analysis for incipient fault diagnosis in oil-immersed transformers,", Expert Systems with Applications, vol. 36, issue 2, part 1, 2009, doi: 10.1016/j.eswa.2007.11.019.

[22] D. Paul, A. K. Goswami, R. L. Chetri, R. Roy and P. Sen, "Bayesian Optimization-Based Gradient Boosting Method of Fault Detection in Oil-Immersed Transformer and Reactors," IEEE Transactions on Industry Applications, vol. 58, no. 2, pp. 1910-1919, March-April 2022, doi: 10.1109/TIA.2021.3134140.

[23] D. Zhang et al., "A bi-level machine learning method for fault diagnosis of oil-immersed transformers with feature explainability," International Journal of Electrical Power & Energy Systems, vol. 134, 107356, 2022, doi: 10.1016/j.ijepes.2021.107356.

[24] H. Besharatifard, S. Hasanzadeh, E. Heydarian-Forushani, H.H. Alhelou, P. Siano, "Detection and Analysis of Partial Discharges in Oil-Immersed Power Transformers Using Low-Cost Acoustic Sensors, " Applied Sciences, vol. *12*, no. 6, pp. 3010, 2022, doi: 10.3390/app12063010.

[25] J. Liu et al., "Moisture Diagnosis of Transformer Oil-Immersed Insulation With Intelligent Technique and Frequency-Domain Spectroscopy," IEEE Transactions on Industrial Informatics, vol. 17, no. 7, pp. 4624-4634, July 2021, doi: 10.1109/TII.2020.3014224.

[26] M. Lin, L. Chen and C. Yu, "A Methodology for Diagnosing Faults in Oil-Immersed Power Transformers Based on Minimizing the Maintenance Cost", IEEE Access,vol. 8, pp. 209570-209578, 2020, doi: 10.1109/ACCESS.2020.3038827.

[27] S. Yu, D. Zhao, W. Chen, H. Hou, "Oil-immersed Power Transformer Internal Fault Diagnosis Research Based on Probabilistic Neural Network", Procedia Computer Science, vol. 83, pp. 1327-1331, 2016, doi: 10.1016/j.procs.2016.04.276.

[28] H. Shang, J. Xu, Z. Zheng, B. Qi, L. Zhang, "A Novel Fault Diagnosis Method for Power Transformer Based on Dissolved Gas Analysis Using Hypersphere Multiclass Support Vector

Machine and Improved D–S Evidence Theory," Energies, 2019, 12, 4017, doi: 10.3390/en12204017.

[29] A. Bracale, G. Carpinelli, M. Pagano and P. De Falco, "A Probabilistic Approach for Forecasting the Allowable Current of Oil-Immersed Transformers," IEEE Transactions on Power Delivery, vol. 33, no. 4, pp. 1825-1834, Aug. 2018, doi: 10.1109/TPWRD.2018.2791181.

[30] L. Jin, D. Kim, A. Abu-Siada and S. Kumar, "Oil-Immersed Power Transformer Condition Monitoring Methodologies: A Review" Energies, 2022, 15, 3379, doi: 10.3390/en15093379.

[31] A. Abdali, A. Abedi, K. Mazlumi, A. Rabiee and J. M. Guerrero, "Novel Hotspot Temperature Prediction of Oil-Immersed Distribution Transformers: An Experimental Case Study," IEEE Transactions on Industrial Electronics, vol. 70, no. 7, pp. 7310-7322, July 2023, doi: 10.1109/TIE.2022.3206690.

[32] M. Badar, P. Lu, Q. Wang, T. Boyer, K. P. Chen and P. R. Ohodnicki, "Real-Time Optical Fiber-Based Distributed Temperature Monitoring of Insulation Oil-Immersed Commercial Distribution Power Transformer," IEEE Sensors Journal, vol. 21, no. 3, pp. 3013-3019, 1 Feb.1, 2021, doi: 10.1109/JSEN.2020.3024943.

[33] J. Ruan, Y. Deng, D. Huang, C. Duan, R. Gong, Y. Quan, Y. Hu, and Q. Rong, "HST calculation of a 10 kV oil-immersed transformer with 3D coupled-field method," IET Electric Power Applications, vol.14, pp. 921-928, 2020, doi: 10.1049/iet-epa.2019.0469.

[34] Y. Deng et al., "A Method for Hot Spot Temperature Prediction of a 10 kV Oil-Immersed Transformer," IEEE Access, vol. 7, pp. 107380-107388, 2019, doi: 10.1109/ACCESS.2019.2924709.

[35] C. Gezegin, O. Ozgonenel and H. Dirik, "A Monitoring Method for Average Winding and Hot-Spot Temperatures of Single-Phase, Oil-Immersed Transformers," IEEE Transactions on Power Delivery, vol. 36, no. 5, pp. 3196-3203, Oct. 2021, doi: 10.1109/TPWRD.2020.3035842.

[36] O. Laayati, M. Bouzi and A. Chebak, "Design of an oil immersed power transformer monitoring and self diagnostic system integrated in Smart Energy Management System," 2021 3rd Global Power, Energy and Communication Conference (GPECOM), Antalya, Turkey, 2021, pp. 240-245, doi: 10.1109/GPECOM52585.2021.9587640.

[37] M. K. Pradhan and T. S. Ramu, "On the estimation of elapsed life of oil-immersed power transformers," IEEE Transactions on Power Delivery, vol. 20, no. 3, pp. 1962-1969, July 2005, doi: 10.1109/TPWRD.2005.848663.

[38] O. Yaman and Y. Biçen, "An Internet of Things (IoT) based Monitoring System for Oil-immersed Transformers," Balkan Journal of Electrical and Computer Engineering , vol. 7, no. 3, pp. 226-234, 2019, doi: 10.17694/bajece.524921.

[39] I. Daminov, A. Prokhorov, R. Caire, M-C. Alvarez-Herault, "Energy limit of oil-immersed transformers: A concept and its application in different climate conditions," IET Generation, Transmission & Distribution, vol. 15, pp. 495–507, 2021, doi:10.1049/gtd2.12036.

[40] M. Kharezy, H. R. Mirzaei, Y. Serdyuk, T. Thiringer and M. Eslamian, "A Novel Oil-Immersed Medium Frequency Transformer for Offshore HVDC Wind Farms," IEEE Transactions on Power Delivery, vol. 36, no. 5, pp. 3185-3195, Oct. 2021, doi: 10.1109/TPWRD.2020.3035718.

[41] S. Okabe, M. Koto, G. Ueta, T. Saida and S. Yamada, "Development of high frequency circuit model for oil-immersed power transformers and its application for lightning surge analysis," IEEE Transactions on Dielectrics and Electrical Insulation, vol. 18, no. 2, pp. 541-552, April 2011, doi: 10.1109/TDEI.2011.5739460.

[42] W. R. Si, C. Z. Fu, X. T. Wu, X. Zhou, X. G. Li, Y. T. Yu and H. Laurent, "Numerical study of electromagnetic loss and heat transfer in an oil-immersed transformer," Mathematical Problems in Engineering, 1-13, 2020, doi:10.1155/2020/6514650.

[43] X. Jia, M. Lin, S. Su, Q. Wang and J. Yang, "Numerical study on temperature rise and mechanical properties of winding in oil-immersed transformer," Energy, vol. 239, 121788, 2022, doi: 10.1016/j.energy.2021.121788.

[44] Y. Zhang, S. L. Ho and W. Fu, "Applying Response Surface Method to Oil-Immersed Transformer Cooling System for Design Optimization," IEEE Transactions on Magnetics, vol. 54, no. 11, pp. 1-5, Nov. 2018, Art no. 8401705, doi: 10.1109/TMAG.2018.2840337.

[45] R. Ni et al., "A temperature calculation method of oil immersed transformer considering delay effects and multiple environmental factors." Electric Power Systems Research, vol. 213, 108260, 2022, doi: 10.1016/j.epsr.2022.108260.

[46] S. V. Kulkarni and S. A. Khaparde, "Transformer Engineering: Design and Practice", by Marcel Dekker , 2004.

[47] S. Nasar, "Electric Machines and Electromechanics", 2nd ed., McGraw-Hill, 1997.

[48] A. E. Fitzgerald, C. Kingsley and S. D. Umaos, "Electric Machinery", 6th ed., McGraw-Hill, 2003.